NUCLEAR EXCHANGE ENERGY AND ISOTOPIC PHASE SEPARATION IN SOLID HELIUM

By
MICHAEL FRANCIS PANCZYK

A DISSERTATION PRESENTED TO THE GRADUATE COUNCIL OF
THE UNIVERSITY OF FLORIDA
IN PARTIAL FULFILLMENT OF THE REQUIREMENTS FOR THE
DEGREE OF DOCTOR OF PHILOSOPHY

UNIVERSITY OF FLORIDA
1968

69-5397

PANCZYK, Michael Francis, 1938-

NUCLEAR EXCHANGE ENERGY AND ISOTOPIC PHASE SEPARATION IN SOLID HELIUM.

The University of Florida, Ph.D., 1968
Physics, solid state

University Microfilms, Inc., Ann Arbor, Michigan

For My *Delightful* Wife,

MARY

ACKNOWLEDGMENTS

I wish to express my sincere appreciation to those individuals listed below for generously contributing both their time and talents to this work.

Dr. E. D. Adams suggested this investigation and provided continual guidance throughout its entire development.

Mr. R. A. Scribner made many valuable contributions to the design and construction of the apparatus and also spent many hours helping take the data. Dr. G. C. Straty contributed his vast technical knowledge to this work and is responsible for the particular design of the strain gauge used in these experiments. Dr. J. R. Gonano often participated in many helpful discussions concerning the interpretation of the experimental results. Messers. D. C. Heberlein and J. W. Philp were frequently called upon to assist me and always did so cheerfully. Mr. B. McDowell often worked long hours to provide the copious quantities of liquid helium necessary to carry on this investigation.

Finally, I wish to express my sincere appreciation to my wife, Mary, for her patience and understanding during what has been a long and at times frustrating graduate career.

TABLE OF CONTENTS

LIST OF FIGURES

Abstract of Dissertation Presented to the Graduate Council
in Partial Fulfillment of the Requirements for the Degree of
Doctor of Philosophy

NUCLEAR EXCHANGE ENERGY AND ISOTOPIC PHASE SEPARATION IN SOLID HELIUM

By

Michael Francis Panczyk

March, 1968

Chairman: Dr. E. Dwight Adams
Major Department: Physics

By making use of a sensitive capacitance type strain gauge, we have investigated the nuclear exchange energy and isotopic phase separation in solid helium mixtures containing 20, 600, and 1600 ppm He^4. Measurements of the pressure versus temperature for constant volume samples between 22.8 and 24.2 cm^3/mole have been made down to 20 m°K, and show the expected T^{-1} dependence due to nuclear spin ordering at low temperatures. The values of the nuclear exchange energy were obtained from the slopes of the P versus T^{-1} curves by means of a self-consistent procedure. The magnitude of the exchange energy, $|J|/k$, is about 0.7 m°K at a molar volume of 24 cm^3/mole and decreases with increasing density approximately as $\frac{d\ln|J|}{d\ln V} = 16.4$. The corresponding magnetic transition temperature varies from 2.4 m°K at 24.2 cm^3/mole down to 0.9 m°K at 22.8 cm^3/mole. Since the data were obtained in a temperature range well below the isotopic phase separation temperature of the three mixtures, the values of $|J|$ reported here are those of a very pure He^3 solid.

The isotopic phase separation in the two samples containing 600 and 1600 ppm He^4 has been detected by observing the increase in pressure which occurs as the mixture separates into two enriched phases.

For the 600 ppm sample this excess pressure is $\simeq 3 \times 10^{-3}$ atm, while for the 1600 ppm sample it is $\simeq 9 \times 10^{-3}$ atm. The corresponding phase separation temperatures, at a molar volume of 24.0 cm^3/mole, are approximately 0.108°K and 0.119°K respectively. A brief investigation of the density dependence of the phase separation phenomenon indicates that both the excess pressure and the phase separation temperature decrease with increasing density.

A discussion of the assumptions and approximations in the theory of "Quantum Crystals" formulated by Nosanow has also been given. A comparison between these theoretical calculations and our experimental results for the exchange energy and its volume dependence indicates that while this theory is qualitatively correct, refinements must be made in order to obtain quantitative agreement with existing experimental data.

CHAPTER I

INTRODUCTION

Helium exists in two stable isotopic forms, He^3 and He^4. He^3 atoms have a spin of 1/2 and hence are treated theoretically by Fermi-Dirac statistics, while He^4 atoms have a spin equal to zero and thus follow a Bose-Einstein distribution law. Since the electrostatic interaction between two He^4 atoms or two He^3 atoms is approximately the same, these isotopes and mixtures of various concentrations provide excellent examples for studying the effects of quantum statistics on the macroscopic properties of systems.

One of the most interesting properties of both the pure isotopes and mixtures is that they remain liquids down to the absolute zero of temperature. This is a consequence of the weak interatomic forces and the small mass of the helium atoms. Pressures of the order of 25 atmospheres are required to bring about the liquid-solid transition. Liquid He^4 has been studied extensively for about fifty years. Most of the research has centered on the properties of the superfluid phase. F. London[1] pointed out that the existence of this phase is closely connected with the fact that the He^4 atom is a boson. Liquid He^3, which is a simple fermion system, exhibits no such superfluid phase, although the possibility of a superfluid transition similar to that occurring in the electron gas in metals has been proposed by several authors.[2,3,4] Experimental investigations of the nuclear magnetic

susceptibility[5,6,7] and spin diffusion coefficient[8] of liquid He^3 indicate that the magnetic properties of the system are in excellent agreement with the theoretical predictions of Landau.[9] The agreement with respect to other properties of the liquid, however, is not quite so good. In particular, recent specific heat measurements[8,10] to 3 m°K do not exhibit a linear dependence on the temperature as one would expect on the basis of Landau's Fermi liquid theory. Thus it appears that additional information about the liquid is needed in order to determine the degree of validity of Landau's approach. In particular, measurements of the isobaric thermal expansion coefficient to temperatures of a few millidegrees are very desirable.

The melting line of He^3 is of particular interest because it exhibits a deep minimum. Although this phenomenon is unusual, since it implies that the solid possesses a greater degree of disorder than liquid, its existence was predicted by Pomeranchuk[11] before it was actually observed in the experiments of Baum, et al.[12] Pomeranchuk argued that the nuclear spins in the solid should be randomly distributed down to temperatures of a few microdegrees, and hence contribute Rln2 to the total entropy. Since the entropy of the liquid is known to fall below this value at about 0.32°K, there should be a change in sign of $(S_\ell - S_s)$ at this temperature and by the Clausius-Clapeyron equation $\frac{dP}{dT}$ should be negative. Although it is now expected that the exchange interaction in the solid near the melting curve will produce nuclear spin alignment in the millidegree rather than the microdegree region, this temperature range is still considerably below 0.32°K, so that Pomeranchuk's original argument for the existence of the minimum remains at least qualitatively correct. The absolute value of $\frac{dP}{dT}$ cannot

continue to increase at temperatures very close to absolute zero since the Nerst Theorem implies that $\left|\frac{dP}{dT}\right| = 0$ at $T = 0$. Recent strain gauge measurements by Scribner, et al.[13] locate the minimum at a temperature of 0.318°K and a pressure of 28.93 atm. These measurements were carried down to 0.017°K and at this temperature $\left|\frac{dP}{dT}\right|$ is still increasing. At the present time it is expected $\left|\frac{dP}{dT}\right|$ will reach a maximum value at about 7 m°K and again become zero at approximately 0.5 m°K.

The properties of the solid phase of helium have not received as much attention as those of the liquid. The experiments of Grilly and Mills[14] revealed the existence of two solid phases of He^3 having a triple point with the liquid at $T = 3.148$°K and $P = 135.9$ atm. X-ray diffraction experiments[15] showed that the crystal structure of the low pressure phase was body-centered-cubic (bcc) while the higher pressure phase was hexagonal-close-packed (hcp). Recent pressure measurements by Straty and Adams[16] showed that below 1°K, the bcc-hcp phase boundary is horizontal at a pressure of about 105 atm. Further x-ray work by Schuch and Mills[17] and by Franck[18] revealed the existence of a third solid phase above $T = 17.78$°K and $P = 1608$ atm. The crystal structure of this phase is cubic-close-packed (ccp). Solid He^4 is also found to exist in these three crystal structures, although the details of the PVT relations of the two solids are somewhat different. The fact that low pressure solid He^3 exists in a body-centered-cubic structure is somewhat unusual since the stable structure for most dielectric solids is cubic-close-packed. Nosanow[19] has demonstrated that the existence of solid helium in the bcc phase is due to the strong short range correlations which arise from the large amplitude zero point motion of the atoms, and hence is a manifestation of the quantum nature of the solid.

Recent heat capacity experiments by Swenson and co-workers[20] and by Pandorf and Edwards,[21] along with the pressure measurements of Straty and Adams,[16] show that above 0.3°K, these properties of the solid are determined principally by the phonons with almost no contribution from the nuclear spin system. This situation cannot continue to very low temperatures since the contribution to the free energy from the phonons decreases while that from the spins increases. As mentioned previously Pomeranchuk[11] originally predicted that the temperature range in which the spin system would determine the properties of the solid should be around a few microdegrees. He based this prediction on the idea that the He^3 atoms in the solid are tightly bound to well separated lattice sites, and hence exchange effects are negligible. Bernardes and Primakoff[22] later pointed out that the large amplitude zero point motion of the He^3 atoms produces considerable overlap of the wave functions of neighboring atoms, and hence exchange effects in the solid are very important. They developed a theory for the ground state of solid He^3 which predicted that antiferromagnetic spin alignment should occur in the low density solid at temperatures of a few hundredths of a degree. More recent calculations by Nosanow[19] indicate that the exchange energy is not quite as large as originally estimated by Bernardes and Primakoff. Nosanow predicts that the magnetic ground state is still antiferromagnetic but that the Néel temperature is approximately 0.2 m°K.

There are many reasons why the nuclear magnetic properties of solid He^3 have received so much attention. One of the most important is the absence of any electronic contribution to the magnetic moment of the atom. Also, since it forms a simple dielectric solid containing

localized spin 1/2 particles, He^3 represents an ideal substance in which to test the various theories of magnetism. From an experimental point of view, the large compressibility of the solid allows one to study the magnetic properties over a wide range of densities by application of modest pressures.

Early experimental attempts to measure the exchange energy in the solid were focused mainly on the nuclear magnetic susceptibility[23] and the specific heat.[24] These early experimental results were inadequate either because of sizable amounts of He^4 impurities or because the measurements were not extended to low enough temperatures. Nuclear susceptibility measurements are very attractive because they allow both the sign and magnitude of the exchange energy, J, to be determined from a single measurement. However, since the Néel temperature in the solid is expected to be of the order of a few millidegrees, it is necessary to make susceptibility measurements to temperatures around 0.02°K and lower to determine J accurately. At these temperatures, especially for the higher densities, measurements become very difficult because of the long thermal equilibrium times between the nuclear spin system, the lattice, and the thermometer. Nevertheless, susceptibility experiments have been performed by Thomson, Meyer, and Dheer[25] to temperatures down to 0.07°K. Their results indicate that the exchange energy is negative, and the corresponding Néel temperature, T_N, is less than 0.02°K for molar volumes greater than 22.4 cm^3/mole. At higher densities, they found a systematic increase in T_N to a value of 0.1°K at a molar volume of 19.5 cm^3/mole. These higher density results were regarded as very tentative however, and may be due to non-equilibrium effects which arise from the He^4 impurities present in the

He^3. These nonequilibrium effects were more apparent in the susceptibility measurements made on the 1% He^4 sample also studied by Thomson, et al.,[25] and are discussed in some detail by them.

Two technical problems make the determination of the exchange energy from specific heat data difficult. The first is the large contribution to the specific heat from isotopic phase separation of He^4 impurities present in the He^3. This was first observed by Edwards, et al.[24] in experiments designed to determine the nuclear spin contribution to the specific heat. These experimenters found a large anomaly in the heat capacity of solid mixtures which suggested that at low temperatures the mixture separates into two phases, one rich in He^3 and the other in He^4. These measurements also indicate that the phase separation line is symmetric about a concentration of 50%, and that the two isotopes will be completely separated at 0°K. The problems presented by the isotopic separation of the He^4 atoms could presumably be surmounted by either using very pure He^3 gas, or lowering the temperature to a region where the phase separation contribution to the specific heat is small. This brings us to the second problem; namely, that as the temperature is reduced, the specific heat of the solid sample becomes less than that of the cerium magnesium nitrate thermometer. This means that the background specific heat of the calorimeter is greater than that of the He^3 sample, and this situation greatly reduces the accuracy with which one can obtain the exchange energy from the experimental data.

Thus far, the most successful determinations of $|J|$ and its volume dependence have been derived from nuclear magnetic relaxation measurements of the spin-lattice and spin-spin relaxation times. Although

other experimenters have also made measurements, the most comprehensive studies have been performed by Richardson, Hunt, and Meyer[26] at Duke and by Richards, Hatton, and Gifford[27] at Oxford. These experimenters find that in the low density bcc phase, the exchange energy $|J|/k$ is approximately 1 m°K and decreases with increasing density. The NMR data also indicate that the value of J depends very strongly on the concentration of the He^4 impurities present in the sample. Although these measurements are by no means conclusive, it appears that the exchange energy is much larger in impure samples than in the relatively pure ones.

The main advantage that magnetic relaxation experiments have over the previously mentioned thermodynamic ones, is that the exchange energy can be determined from data obtained above 0.3°K. This temperature region is within range of a helium three refrigerator and hence no paramagnetic refrigerant is necessary. Furthermore, the thermal time constants between the spins, lattice, and thermometer remain reasonably short above 0.3°K. The principal objection to determinations of the exchange energy based solely on T_1 and T_2 data is that these relaxation times are related to J by a rather complex formalism which has undergone considerable numerical revision. These measurements thus constitute a somewhat indirect determination of the exchange energy and additional thermodynamic data are very desirable.

In this work we report the first direct determination of $|J|$ and its volume dependence for molar volumes between 22.8 and 24.2 cm^3/mole. The values of $|J|$ are obtained from measurements of the internal pressure and temperature of constant volume samples. In addition we have also made the first pressure measurements of the isotopic phase separation temperature for samples containing 600 and 1600 ppm He^4.

In the following chapter we discuss the Nosanow theory[19] of "Quantum Crystals" and also obtain an approximate equation of state for the solid at low temperatures. This equation of state relates the exchange energy and its volume dependence to the internal pressure and temperature of the solid, and can be used to extract $|J|$ from the P, T data. In addition we will also obtain an expression for the increase in pressure due to the isotopic phase separation, based upon the assumption that the He^3 and He^4 atoms mix together in a completely random fashion.

In Chapter III we describe the apparatus used in these experiments. In particular we will discuss in detail the potassium chrome alum salt system used to lower the temperature to a region where the effects of the spin system become observable, and the capacitive strain gauge used to measure the small pressure changes produced by the nuclear spin ordering.

In Chapter IV we present our results for the exchange energy and its volume dependence, along with the results derived from the NMR experiments. A comparison will be made between these experimental data and the theoretical calculations of Nosanow and his co-workers.[19,28] We also present results for the isotopic phase separation temperature, energy of mixing, and equilibrium time constant for the samples 600 and 1600 ppm He^4. The volume dependence of these quantities is also discussed.

Finally in the last chapter we will give a brief summary of the present situation with respect to the exchange energy and phase separation, and suggest some future experiments whose results should enhance our understanding of solid helium.

CHAPTER II

THEORETICAL TREATMENTS OF SOLID HE^3

A. Introductory Remarks

In this chapter we shall discuss in detail two theoretical treatments of the ground state of solid He^3. For want of better names, we refer to these as the microscopic and thermodynamic approaches to the problem. In a microscopic theory one is interested in obtaining values for the various properties of the system such as the ground state energy and nuclear exchange energy from a solution of the many body Schroedinger equation, while in a thermodynamic theory one regards these quantities as experimentally determined parameters and attempts to obtain an approximate equation of state for the system. Although there have been several microscopic theories[22,29] proposed in recent years, we shall discuss in detail only the most recent work of Nosanow and his co-workers[19,28] since it appears to represent the "state of the art" as it exists today. Goldstein[30] has devoted considerable attention to the thermodynamic properties of both liquid and solid helium, and the macroscopic equation of state which we shall develop is similar to that appearing in his most recent work. Before discussing these theoretical attempts to calculate the ground state properties of the solid, however, a few words concerning the physical origin of the exchange energy seem appropriate.

B. Physical Origin of the Exchange Energy

When Weiss[31] proposed his molecular field theory in 1907, it was assumed that the ordinary magnetic dipole-dipole interaction between neighboring atoms was responsible for the observed spontaneous magnetization in ferromagnets. However, it soon became evident that the observed transition temperatures were much too high to be explained on the basis of a simple dipolar interaction which predicts a transition temperature $T_c \sim \mu^2/R^2$, where μ is the net magnetic moment, and R the distance between neighboring atoms. For iron, the observed transition temperature is $\sim$ 1000°K, while the temperature calculated from the dipolar interaction is about 1°K. Thus to account for the experimental data, it was necessary to find an interaction which is about a thousand times stronger than the magnetic dipole one. The discovery of this unknown interaction had to wait about twenty years for Schroedinger and Heisenberg to develop quantum mechanics. Shortly after the formulation of this theory, Heisenberg[32] applied it to the problem of ferromagnetism. He showed that the interaction responsible for spontaneous magnetization was truly quantum mechanical, being a direct result of the symmetry restrictions placed on the wave function by the Pauli exclusion principle.

To illustrate the important role that the exclusion principle plays in determining the ground state energy of a system of fermions, it is useful to consider the simple example of two spin 1/2 particles interacting with each other through a potential $V(r_{12})$. The Hamiltonian, omitting the dipole-dipole term, is given by

$$H(1,2) = -\frac{\hbar^2}{2m}(\nabla_1^2+\nabla_2^2)+V(r_{12}). \qquad (2.1)$$

Consider two cases:

CASE I. The particles are distinguishable so that the restrictions of the Pauli principle need not be considered. A suitable wave function for the two particles is then

$$\psi(\vec{r}_1,\vec{r}_2) = \phi_i(\vec{r}_1)\phi_j(\vec{r}_2) \tag{2.2}$$

where i and j refer to the i^{th} and j^{th} single particle eigenstates. The total energy will then be

$$E_o = E_i+E_j+\int\phi_i^*(\vec{r}_1)\phi_j^*(\vec{r}_2)V(r_{12})\phi_i(\vec{r}_1)\phi_j(\vec{r}_2)d\vec{r}_1d\vec{r}_2, \tag{2.3}$$

and is independent of the relative spin orientations of the particles.

CASE II. The particles are indistinguishable so that the exclusion principle requires the wave function to be antisymmetric. A linear combination of the ϕ_i and ϕ_j which satisfies this requirement is

$$\psi(\vec{r}_1,\vec{r}_2) = \frac{1}{\sqrt{2}}[\phi_i(\vec{r}_1)\phi_j(\vec{r}_2)\pm\phi_i(\vec{r}_2)\phi_j(\vec{r}_1)]S(\vec{s}_1,\vec{s}_2) \tag{2.4}$$

where $S(\vec{s}_1,\vec{s}_2)$ is the singlet spin function if the positive sign is used, and the triplet spin function if the negative sign is used. The total energy is no longer degenerate, but instead is given by

$$E_o' = E_o\pm\int\phi_i^*(\vec{r}_1)\phi_j^*(\vec{r}_2)V(r_{12})\phi_i(\vec{r}_2)\phi_j(\vec{r}_1)d\vec{r}_1d\vec{r}_2 \tag{2.5}$$

where the additional term is called the exchange energy J_{ij} of the two spins in states i and j. The total energy is now seen to depend upon the relative spin orientations of the two particles.

The essential difference between Cases I and II lies in the distinguishability of the particles, which in turn is determined by their spacial motions. When the volumes spanned by particles 1 and 2 have a

common region, they are indistinguishable and we get $J_{ij} \neq 0$, while if these volumes do not overlap the particles are distinguishable and $J_{ij} = 0$. The size of the nuclear exchange energy in solids is thus seen to be a measure of how large an overlap there is between wave packets describing the vibrations of neighboring atoms. In solid He^3 the weak interatomic forces and small mass combine to produce large amplitude zero point vibrations of the atoms about their equilibrium positions, and hence one might expect solid He^3 to exhibit sizeable nuclear exchange effects.

In 1929, Dirac[33] showed that for localized spins in orthogonal orbitals the exchange energy can be written as

$$H_{ex} = -2 \sum_{i<j}^{N} J_{ij} \vec{S}_i \cdot \vec{S}_j . \tag{2.6}$$

This is the famous Heisenberg Hamiltonian developed by Dirac and first used extensively by Van Vleck.[34] When written in this form, the exchange energy appears to result from a direct two body spin-spin interaction. Also one sees that the magnetic ground state (ferro or antiferromagnetic) will be determined by the sign of J_{ij}. If $J_{ij} < 0$ antiparallel spin alignment will be favored and the ground state of the system will be antiferromagnetic, while if $J_{ij} > 0$ the ground state will be ferromagnetic. Furthermore, when expressed in this form it is immediately evident that the exchange energy represents the difference between the singlet and triplet state energies. Finally, this form is very attractive because it allows the powerful spin operator formalism to be applied to the theory of magnetism. Perhaps because of the clarity with which Eq.(2.6) defines the exchange energy and magnetic ground state of a system, misconceptions about the microscopic

origin of the exchange interaction have arisen. It is important, therefore, to realize that exchange forces result from the symmetry requirements placed on the wave function by the Pauli exclusion principle, not from any direct spin-spin coupling. Having concluded this brief interlude on the physical origin of the exchange energy, we may now discuss some of the theories of the ground state of solid He^3.

C. Microscopic Theory

As previously mentioned, any attempt to calculate the ground state energy and wave function for solids from first principles is faced with the problem of finding a solution to the many body problem. This is a most difficult problem and can be solved only if approximations are made. The nature of these approximations is generally determined by the specific system under consideration. For solids of heavy atoms, the root mean square deviation of the particles about their equilibrium positions is small so that the harmonic approximation for the potential, along with uncorrelated single particle wave functions may be used. Such calculations for solid He^3 have been spectacularly unsuccessful. Nosanow and Shaw[35] have calculated the ground state energy of noble gas solids, using uncorrelated single particle wave functions and a Lennard-Jones 6-12 potential. For the other heavy noble gas solids, the theoretical value of the cohesive energy is within the experimental limits, while for solid helium, the calculated value is of the order of 30 cal/mole, while experimental value is about $-4.5 \pm .5$ cal/mole. From this type of calculation it is evident that uncorrelated single particle type functions are an inadequate description of the ground state of solid helium. The reason for this inadequacy is that

these functions do not take into account the short range correlations which arise from the very large zero point motion of the atoms.

The first attempt to include these short range correlations into the theory of solid He^3 was made by Bernardes and Primakoff,[22] who made a variational calculation of the ground state energy and wave function. They reasoned that correlations in the motions of pairs of atoms could be accounted for by replacing the true interaction potential by a single parameter effective one. They assumed an analytical form for this effective potential given by

$$V(r,\lambda) = 4\epsilon\left[\left(\frac{\sigma}{r}\right)^{12} - \left(\frac{\sigma}{r}\right)^{6}\right]e^{-\lambda r^{-10}}. \qquad (2.7)$$

The parameter λ was determined by fitting the known ground state energy and root mean square deviation for crystalline He^4. Their calculations were approximately correct for the bulk properties of the solid, but vastly overestimated the nuclear exchange energy. It is now realized that due to the differences in crystal structure and statistics the effective potential between nearest neighbor atoms of the two solids is significantly different. The exchange integral is very sensitive to the variations in the tail of the wave function which is determined primarily by the repulsive part of the potential. Therefore, any effective potential determined from He^4data will not be accurate enough to calculate quantitatively the exchange energy for solid He^3. Despite this shortcoming in their approach, Bernardes and Primakoff were able to correctly predict that both J and $\frac{dJ}{dP}$ would be negative in the body-centered-cubic phase. Their value for J is about two orders of magnitude too large and the pressure dependence of J as estimated from variation of λ with pressure is also much too large.

Nosanow and his co-workers[19,28] have made a systematic study of the ground state properties of quantum crystals by employing a variational calculation of the energy based on a cluster expansion technique. This group succeeded in calculating the ground state pressure and energy of solid helium to a few percent, while obtaining reasonable agreement with the available experimental values for the exchange energy. Since the Nosanow treatment is the most comprehensive and gives the best agreement with all the available experimental data, a discussion of the assumptions and approximations of this theory will be given.

Nosanow's Theory of Quantum Crystals

If we consider a system of N particles of mass m interacting with each other through a potential function $V(r_{ij})$, the Schrödinger equation is

$$\left[-\frac{\hbar^2}{2m}\sum_{i=1}^{N}\nabla_i^2+\sum_{i<j}V(r_{ij})\right]\psi(\vec{r}_1,\vec{r}_2\ldots\vec{r}_N)=E\psi(\vec{r}_1,\vec{r}_2\ldots\vec{r}_N). \qquad (2.8)$$

For He^3 the Lennard-Jones 6-12 potential

$$V(r_{ij})=4\epsilon\left[\left(\frac{\sigma}{r_{ij}}\right)^{12}-\left(\frac{\sigma}{r_{ij}}\right)^{6}\right] \qquad (2.9)$$

gives an adequate representation of the interatomic forces. In Eq.(2.9), ϵ and σ are constants determined from the low temperature gas phase data and have values of 10.22°K and 2.55 Å respectively.

The effects of short range correlations are included in the function ψ by taking it to have the form

$$\psi(\vec{r}_1\ldots\vec{r}_i\ldots\vec{r}_N)=\prod_{i=1}^{N}\phi_i(\vec{r}_i-\vec{R}_i)\prod_{i<j}^{N}f(r_{ij}), \qquad (2.10)$$

in this expression $\vec{R}_i$ is the coordinate of the i^{th} lattice site, $\vec{r}_i$ is

the position vector of the i^{th} atom and r_{ij} is the distance between the i^{th} and j^{th} atoms. The function ψ in Eq.(2.10) is not properly symmetrized with respect to an interchange of He^3 atoms and hence cannot adequately describe exchange effects. In the actual calculation, the two body exchange energy is accounted for by using an antisymmetrized two particle wave function constructed from the appropriate linear combination of the $\phi_i(\vec{r}_i-\vec{R}_i)$ and spin functions.

The function $\prod_i^N \phi_i(\vec{r}_i-\vec{R}_i)$ has the normal Hartree form. The boundary conditions are

$$\lim_{r \to 0} \phi(r) = \text{finite} \tag{2.11a}$$

$$\lim_{r \to \infty} \phi(r) = 0 \tag{2.11b}$$

$$\phi(r) \neq 0 \qquad \text{for} \qquad r > R/2, \tag{2.11c}$$

condition (2.11c) permits the wave packets of neighboring He^3 atoms to overlap. Nosanow chooses $\phi(r)$ to have the spherically symmetric form

$$\phi(r) = \exp(-Ar^2/2) \tag{2.12}$$

where A is a variational parameter to be determined. The function $\prod_{i<j} f(r_{ij})$ is introduced to account for the short range correlations in He^3. By the particular functional form chosen, one can see that only two body correlations are to be considered. The boundary conditions on $f(r_{ij})$ are

$$\lim_{r \to 0} f(r) = 0 \tag{2.13a}$$

$$\lim_{r \to \infty} f(r) = \text{constant}. \tag{2.13b}$$

Condition (2.13a) reflects the strong repulsion of He^3 atoms at small distances, while (2.13b) expresses the fact that at large distances the atoms are essentially uncorrelated. One of the analytical forms used by Nosanow for the correlation function is

$$f(r) = \exp\{-K\left[\left(\frac{\sigma}{r}\right)^{12} - \left(\frac{\sigma}{r}\right)^{6}\right]\} \tag{2.14}$$

where K is a variational parameter to be determined. The procedure is to determine A and K by a variation of the energy

$$E_o = \frac{(\psi, H\psi)}{(\psi,\psi)} \tag{2.15}$$

with respect to these parameters.

Up to this point, the main approximation in the theory is the admission of two body correlations only. However due to the presence of the function $\prod_{i<j} f(r_{ij})$, evaluation of $(\psi,H\psi)$ becomes difficult to do without additional approximations. In order to evaluate $(\psi,H\psi)$, Nosanow makes a cluster series expansion of the energy in such a way that each successive term in the expansion makes a decreasing contribution to E_o. It should then be possible to truncate the series after a few terms, provided it converges rapidly.

To make the expansion, it is convenient to introduce the quantity

$$M(\gamma) = (\psi, \exp\gamma H\psi), \tag{2.16}$$

so that

$$E_o = \lim_{\gamma \to 0} \frac{\partial}{\partial\gamma} \ln M(\gamma). \tag{2.17}$$

In the cluster series expansion the $M(\gamma)$ is expressed in the form

$$M(\gamma) = \prod_{n=1}^{N} M_n(\gamma) \tag{2.18}$$

where the only contribution to M_n arises from that volume of phase space where n particles are grouped together in a cluster. Equations (2.16) and (2.17) lead to an expression for the energy, E_o, of the form

$$E_o = \sum_{n=1}^{N} E_{on} \tag{2.19}$$

where the E_{on} give the contribution to the energy of the system from a cluster of n particles. For this series to be rapidly convergent, it is clear that the contributions to E_o from clusters of four or five particles must be much smaller than the single and pair particle energies.

The derivation of the various E_{on} is accomplished by first calculating the $M_n(\gamma)$ and then using the expression $E_{on} = \lim_{\gamma \to 0} \frac{\partial}{\partial \gamma} \ln M_N(\gamma)$. It is quite difficult to do, especially for $n > 2$, and only the results for the special forms of ϕ and f specified above will be presented here. To conform with Nosanow's notation, we need to define the average value of a function $g(\vec{r}_1 \ldots \vec{r}_i \ldots \vec{r}_N)$ over the weight function $\phi(\vec{r}_1 \ldots \vec{r}_i \ldots \vec{r}_N)$ by

$$\langle g(\vec{r}_1 \ldots \vec{r}_i \ldots \vec{r}_N) \rangle \equiv \frac{1}{\omega^N} \int d\vec{r}_1 \ldots \int d\vec{r}_N \Big[|\phi(|\vec{r}_1 - \vec{R}_1|)|^2 \ldots$$

$$|\phi\ |\vec{r}_N - \vec{R}_N|)|^2 g(\vec{r}_1 \ldots \vec{r}_N) \Big], \tag{2.20}$$

$$\langle g(\vec{r}_i, \vec{r}_j) \rangle_x \equiv \frac{1}{\omega^2} \int d\vec{r}_i \int d\vec{r}_j \Big[\phi^*(|\vec{r}_i - \vec{R}_i|) \phi^*(|\vec{r}_i - \vec{R}_j|) \times$$

$$\phi(|\vec{r}_j - \vec{R}_j|) \phi(|\vec{r}_j - \vec{R}_i|) g(\vec{r}_i, \vec{r}_j) \Big], \tag{2.21}$$

where

$$\omega \equiv \int |\phi(|\vec{r}_i - \vec{R}_i|)|^2 d\vec{r}_i. \tag{2.22}$$

The ground state energy is then given by the expression

$$E_0 \simeq E_{01} + E_{02V} + E_{02T} + E_{02J} + E_{03V} + E_{03T}, \tag{2.23}$$

where the various terms have the following forms.

$$E_{01} = \sum_{i=1}^{N} \frac{\int \phi^*(|\vec{r}_i - \vec{R}_i|)\left(-\frac{\hbar^2}{2m}\right)\nabla_i^2 \phi(|\vec{r}_i - \vec{R}_i|) d\vec{r}_i}{\int \phi^*(|\vec{r}_i - \vec{R}_i|)\phi(|r_i - R_i|) d\vec{r}_i} = \frac{3N\hbar}{4}\left(\frac{\hbar A}{m}\right), \tag{2.24}$$

and

$$E_{02V} = \frac{1}{2} \sum_{i,j}{}' \frac{\langle v_{eff}(r_{ij})\rangle}{\langle f^2(r_{ij})\rangle}, \tag{2.25}$$

with

$$v_{eff} = \left(V(r_{ij}) - \frac{h^2}{2m} \nabla^2 \ln f(r_{ij})\right) f^2(r_{ij}). \tag{2.26}$$

$E_{02T} = E_{03T} = 0$ for the particular form of $\phi(r)$ chosen.

$$E_{02J} = \pm \frac{1}{4} \cdot \sum_{i,j}{}' J_{ij} \tag{2.27}$$

where

$$J_{ij} = \left[\frac{-\hbar^2 R^2 A^2}{2m} + \frac{2\langle f^2(r_{ij}) V(r_{ij})\rangle}{\langle f^2 r_{ij}\rangle} \right] \frac{\langle f^2(r_{ij})\rangle_x}{\langle f^2(r_{ij})\rangle} + \frac{2\langle f^2(r_{ij}) V(r_{ij})\rangle_x}{\langle f^2(r_{ij})\rangle} \tag{2.28}$$

has been defined such that J_{ij} is the difference in energy between the singlet and triplet spin states. Finally

$$E_{03V} = \frac{1}{2} \sum_{i,j,k}{}' \frac{\langle f^2(r_{ik}) f^2(r_{jk}) v_{eff}(r_{ij})\rangle}{\langle f^2(r_{ij}) f^2(r_{jk}) f^2(r_{ik})\rangle} - \frac{\langle v_{eff}(r_{ij})\rangle}{\langle f^2(r_{ij})\rangle}. \tag{2.29}$$

The form of each term can be related very nicely to physically intuitive quantities. E_{01} is the single particle contribution to the

energy of the solid. It has been expressed in a form closely resembling the ground state energy of a system of N harmonic oscillators. The second term E_{02V} measures the contribution to the energy produced by the atoms taken in pairs. The Lennard-Jones 6-12 potential however, is replaced by an effective potential which depends upon the form of the short range correlation function $f(r_{ij})$. The term E_{03V} is slightly more general than E_{02V}. It can be considered to be the effective potential energy resulting from all possible interactions involving three particles. Since this includes contributions from two particle interactions already counted in E_{02V}, these must be subtracted out. E_{02J} is the two particle exchange energy and was calculated using a two particle antisymmetric wave function of the form

$$\psi^2(\vec{r}_i,\vec{r}_j) = [\phi(|\vec{r}_i-\vec{R}_i|)\phi(|\vec{r}_j-\vec{R}_j|)\pm\phi(|\vec{r}_i-\vec{R}_j|)\phi(|\vec{r}_j-\vec{R}_i|)]f(r_{ij})S(\vec{s}_i,\vec{s}_j) \quad (2.30)$$

where the plus and minus sign in Eq.(2.30) go with the singlet and triplet spin states respectively. In Eq.(2.28) the term $-\frac{\hbar^2R^2A^2}{2m}\frac{\langle f^2(r_{ij})\rangle_x}{\langle f^2(r_{ij})\rangle}$ is the exchange kinetic energy and is seen to have a negative sign. Further, it turns out to be about three orders of magnitude larger than the second term in brackets. The expression $\frac{2\langle v_{eff}\rangle_x}{\langle f^2(r_{ij})\rangle}$ is the contribution to the exchange integral from effective potential in the overlap region. From Eq.(2.28) one sees that the sign of J will be determined by the relative magnitude of these two terms. If the former term is greater, J will be negative and the magnetic ground state will be antiferromagnetic, while if the latter is greater, J will be positive and the ground state will be ferromagnetic. It is interesting to note that $J_{ij} = 0$ when $\langle f^2\rangle_x$ and $\langle v_{eff}\rangle_x = 0$, that is when there is no overlap of the various ϕ_i.

In Nosanow's 1966 paper, which we shall refer to as N, the basic assumption is that the three body and exchange contributions to the ground state energy are small so that E_0 is approximately given by

$$E_0 \simeq E_{01}+E_{02V}. \tag{2.31}$$

The values of the parameters K and A can then be obtained by minimizing E_0. These values may then be used to calculate the terms, E_{03V} and E_{02J} in the cluster expansion. If these terms are small, the cluster expansion is assumed to converge rapidly.

In a subsequent paper by Hetherington, Mullin, and Nosanow,[28] (HMN) the three body term E_{03V} is included in E_0 and the parameters A and K are chosen to minimize

$$E_0 \simeq E_{01}+E_{02V}+E_{03V}. \tag{2.32}$$

The actual variational calculation itself becomes formally identical with the single particle Hartree calculation of Nosanow and Shaw[35] except that the true interaction potential $V(r_{ij})$ is replaced by an effective potential which is approximately given by

$$v_{eff}(r_{ij}) = f^2(r_{ij})[V(r_{ij})-\frac{\hbar^2}{2m}\nabla^2 \ln f(r_{ij})]. \tag{2.33}$$

When viewed in this manner, the Nosanow approach is seen to be similar to that used by Bernades and Primakoff. Namely, the effects of correlations are taken into account by replacing the true potential by an effective one. However, in the Nosanow theory, v_{eff} is found by minimizing the ground state energy of He^3 while in the Bernades and Primakoff theory, the effective potential was determined from the known ground state properties of He^4. The results of these calculations are summarized in Fig. (1), (2), and (3).

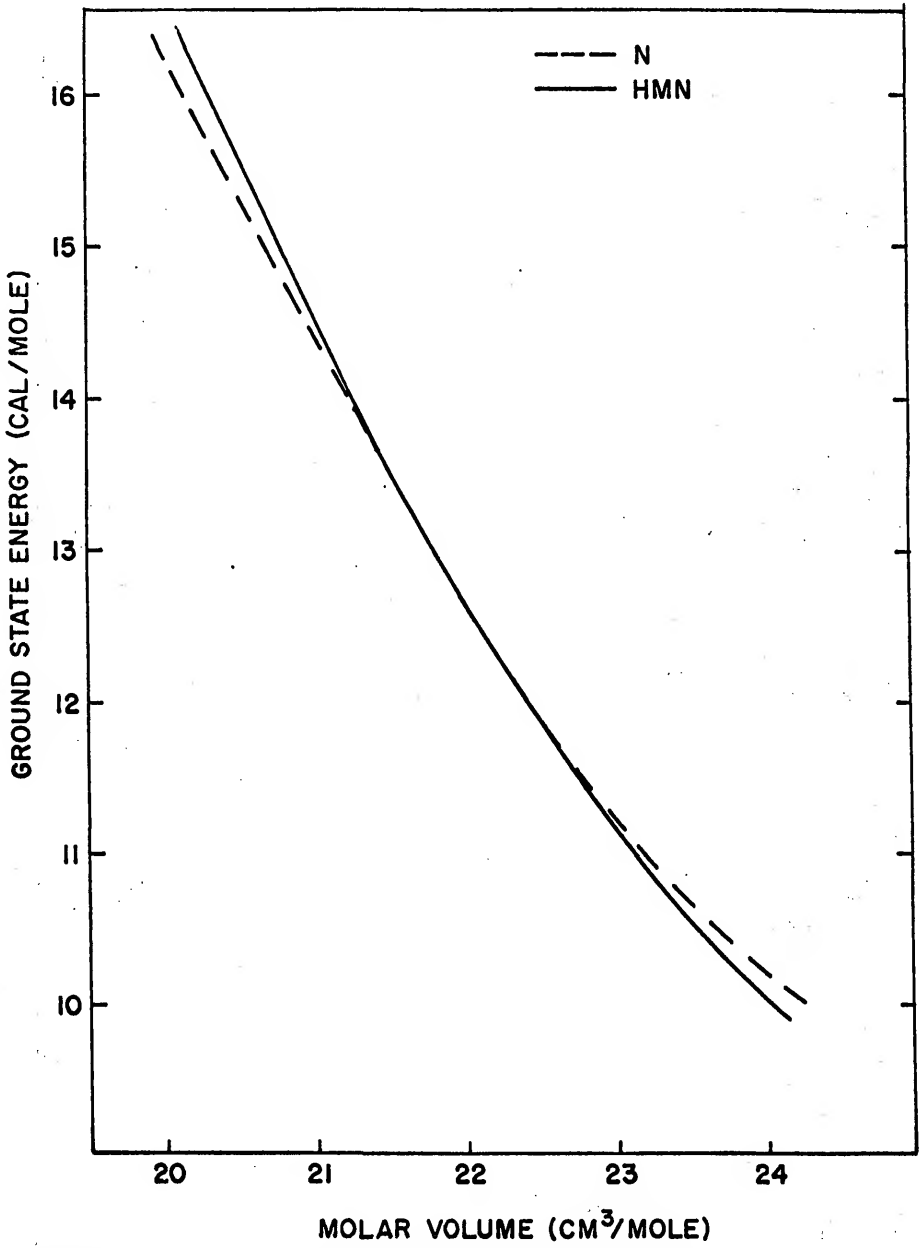

Figure 1. Calculated ground state energy versus molar volume. The dashed curve was obtained by minimizing $E_{01}+E_{02V}$ while the solid curve was obtained by minimizing $E_{01}+E_{02V}+E_{03V}$.

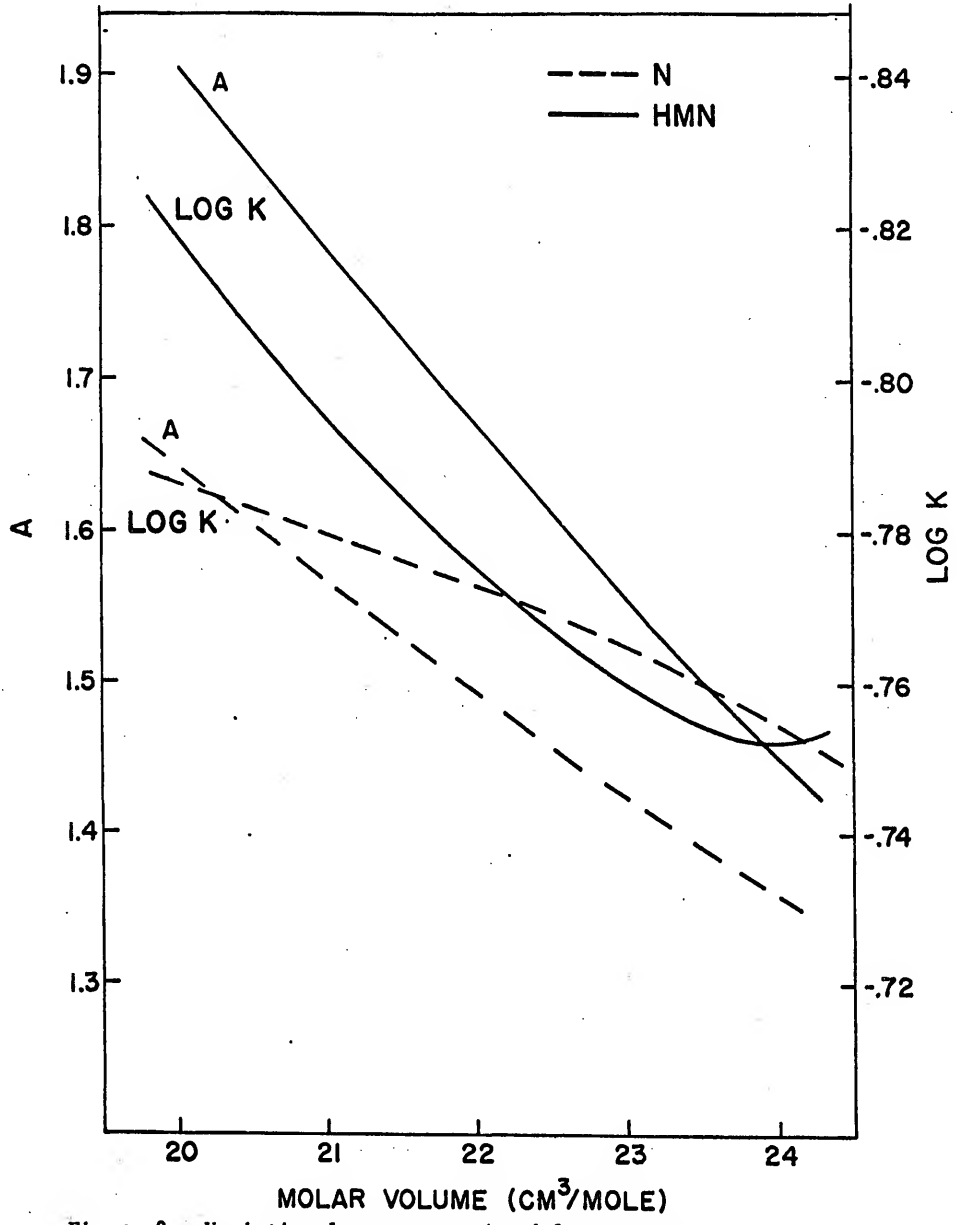

Figure 2. Variational parameters A and log K versus molar volume. The dashed curve gives the parameters that minimize $E_{01}+E_{02V}$, and the solid curve gives those that minimize $E_{01}+E_{02V}+E_{03V}$. Larger values of A correspond to a greater localization of the atoms about their lattice sites.

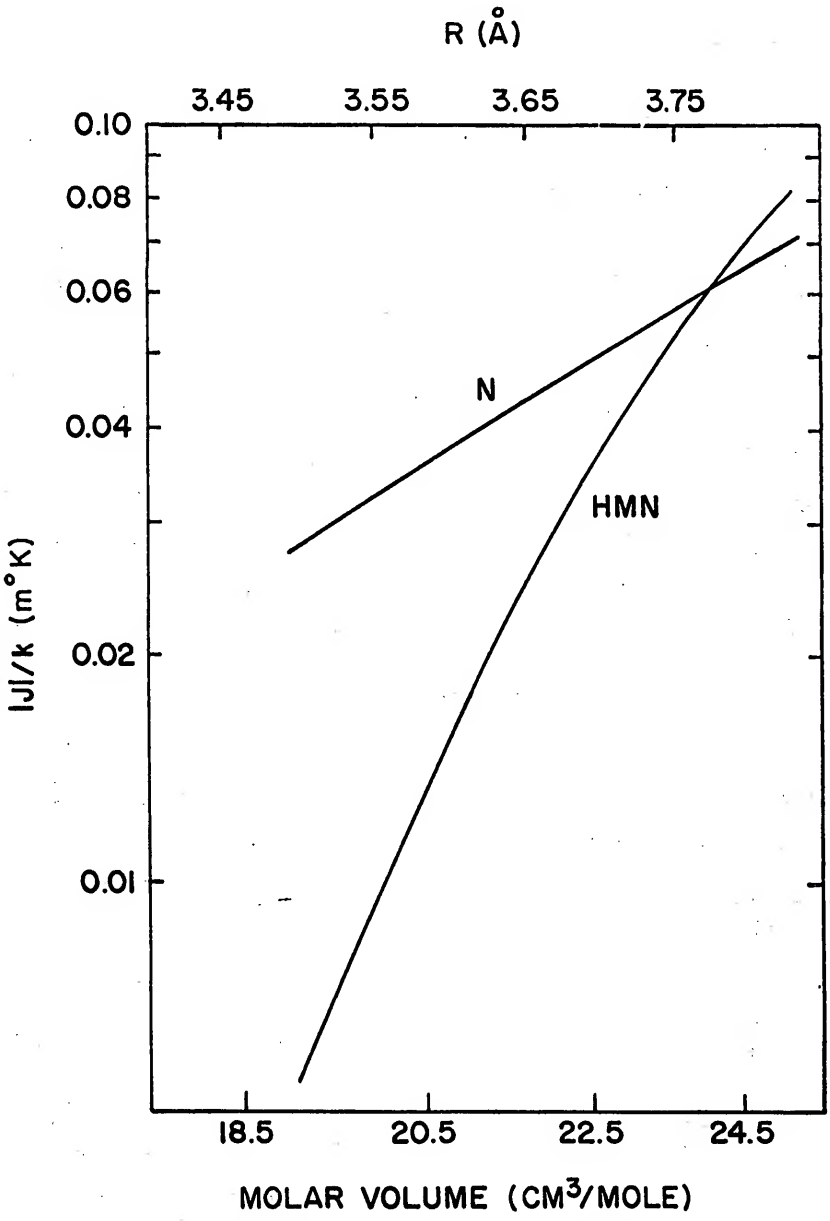

Figure 3. Calculated nuclear exchange energy versus molar volume. Curve N was calculated using the parameters which minimize $E_{01}+E_{02V}$; curve HMN was calculated using those which minimize $E_{01}+E_{02V}+E_{03V}$.

From Fig. (1) we see immediately that the inclusion of the term E_{03V} has only a small effect on the total ground state energy E_0, and thus the truncation of the energy expansion seems valid. Moreover, in HMN, a physical argument based upon the short range nature of the correlation function $f(r_{ij})$ is given which indicates that higher order terms in the cluster expansion will be small. From Fig. (3) however, it can also be seen that while the changes in A and K introduced by the inclusion of E_{03V} in E_0 do not greatly affect the values of the total energy, they do significantly alter both the value and the shape of J(R). This should not be too surprising and can be understood by the following argument. The main contributions to E_0 come from E_{01} and E_{02V}. The former is completely independent of the choice of K and depends only on the width of $\phi(r)$, hence small changes in A will produce only slight variations in E_0. While E_{02V} does depend on both f(r) and $\phi(r)$, the dependence is such that small changes in A and K do not greatly affect E_{02V}. This is because it is related to the average values of f(r) and $\phi(r)$ and not their detailed structure. On the other hand, the quantity

$$J_{ij}(R) \simeq -\frac{\hbar^2R^2A^2}{2m}\frac{\langle f^2(r_{ij})\rangle_x}{\langle f^2(r_{ij})\rangle} + \frac{2\langle v_{eff}(r_{ij})\rangle_x}{\langle f^2(r_{ij})\rangle} \qquad (2.34)$$

depends on a knowledge of the details of both f(r) and $\phi(r)$. In particular, J_{ij} is most sensitive to variations in the wings of $\phi(r)$ since this is where the overlapping occurs. Also, it is expected that J_{ij} should be very sensitive to changes in the function f(r) since it is this function which describes the short range correlations between neighboring atoms. Nosanow and Mullin[28] have investigated the sensitivity of J_{ij} to the function f(r). They varied K from 0.14 to 0.18

and found that J_{ij} changed by a factor of 3 while the energy changed by only 1%. They also changed the first exponent in f(r) from 12 to 8 and found that while J varied by a factor of 4, the total energy changed by only 10%. This sensitivity of J_{ij} and insensitivity of E_0 to slight modifications of the parameters illustrates a basic deficiency in all variational calculations of the exchange energy. Namely, that, although the energy is determined to a few percent, the wave function is not an accurate enough representation of the true ground state function to enable one to calculate accurately the value of the exchange energy.

Before ending this discussion of the Nosanow theory, some consideration should be given to the use of spherically symmetric functions for $\phi(r)$ and f(r). It is known that the low density phase of solid He^3 has a body-centered-cubic crystal structure. This suggests that spherically symmetric functions will be a good representation for the motion of atoms for small values of r. However, for large values of r ($r > \frac{R}{2}$), the cubic symmetry of the lattice must be reflected in the wave function. It is precisely in this region that the overlap integral is large and hence the exchange energy sizeable. It is conceivable, therefore, that the assumption of spherical symmetry introduces an error into the calculations of the exchange integral. Numerical values for $\phi(r)$ have been considered in the theory, and generally speaking they tend to make the exchange energy somewhat larger.

The above remarks are intended only to illustrate some of the problems associated with any theoretical attempt to calculate the exchange energy accurately. In point of fact, the clarity and physical basis for the assumptions and approximations, coupled with the good

agreement between the theoretical calculations of Nosanow and experimental data make this work a significant contribution to the understanding of solid He^3.

D. Thermodynamic Theory

In this section we will obtain an approximate equation of state for a solid composed mainly of He^3 atoms but containing a small amount of He^4 impurities. To do this it is necessary to construct suitable models for the various degrees of freedom of the system. The choice of these models will be based upon both experimental information and theoretical intuition.

The experiments of Edwards, et al.[24] show that below 0.5°K the specific heat of the lattice in the bcc phase can be represented by a Debye term plus a term arising from the phase separation of a regular mixture. We may thus write this contribution to the free energy in the form

$$F_L(x,V,T) = F_D(x,V,T)+F_{PS}(x,V,T)+U_0(x,V). \tag{2.35}$$

In Eq.(2.35) $U_0(x,V)$ is the zero point energy, $F_D(x,V,T)$ and $F_{PS}(x,V,T)$ are the Debye and phase separation contributions to the free energy, and x is the concentration of the He^4 atoms.

Since the exchange energy arises from localized spin 1/2 particles, one should be able to treat the magnetic interactions on the basis of a Heisenberg Hamiltonian of the form

$$H_{ex} = -2 \sum_{i,j} J_{ij}(x,V)\vec{I}_i\cdot\vec{I}_j \tag{2.36}$$

where $J_{ij}(x,V)$ is the exchange integral between nearest neighbor atoms,

and the summation extends over nearest neighbor atoms only. Using this Hamiltonian, one can then calculate a partition function $Q_{ex}(x,V,T)$ from which the magnetic free energy $F_{ex}(x,V,T)$ may be obtained. The total free energy will then be the sum of F_{ex} and F_L and is given by

$$F(x,V,T) = U_0(x,V)+F_D(x,V,T)+F_{PS}(x,V,T)+F_{ex}(x,V,T). \qquad (2.37)$$

The equation of state of the system can then be obtained from the relation

$$P(x,V,T) = -\left[\frac{\partial F(x,V,T)}{\partial V}\right]_{x,T} \qquad (2.38)$$

In order to determine the functions F_D, F_{PS}, and F_{ex} it is useful to divide the temperature scale into three regions as shown below.

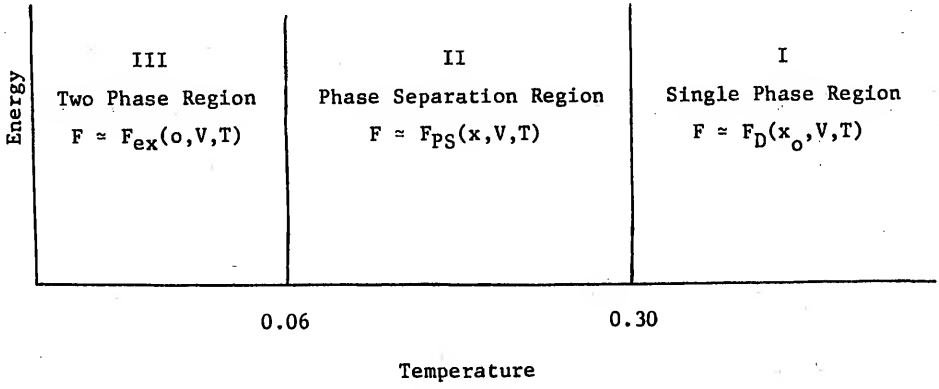

In region I, where $F_D(x,V,T)$ is the main contributor to the energy, the solid exists as a single homogeneous phase having a temperature independent concentration x_o. We may, therefore, write $F_D(x,V,T) = F_D\left|\frac{\theta(x_o,V)}{T}\right|$ where $\theta(x_o,V)$ is the characteristic Debye temperature for the solid. Region II is the isotopic phase separation region. In this temperature range the solid is transformed from a single homogeneous phase of concentration x_o into two separated phases. Initially, the He^4 concentration

of these separated phases varies rapidly with the temperature; however, by the time one reaches 0.06°K, the separation into pure phases is practically completed. Below about 0.06°K, therefore, the solid exists in the form of a large nearly pure He^3 phase in equilibrium with a small He^4 phase. The energy in this range will thus be essentially that of a pure He^3 system. We may then write the magnetic contribution to the energy in the form $F_{ex}(x,V,T) = F_{ex}(o,V,T)$. The total free energy then becomes

$$F(x,V,T) = U_0(V)+F_D\left[\frac{\theta(x_o,V)}{T}\right]+F_{PS}(x,V,T)+F_{ex}(o,V,T). \qquad (2.39)$$

We will now obtain expressions for the various terms in Eq.(2.39). The spin partition function $Q_{ex}(v,T)$ is given formally by the expression

$$Q_{ex}(V,T) = \text{trace } e^{-H_{ex}/kT} = \text{trace } e^{+\frac{2J}{kT}\sum_{i<j}^{N}\vec{I}_i\cdot\vec{I}_j}. \qquad (2.40)$$

Rushbrooke and Wood[36] have made a series expansion of this function in powers of $\frac{J}{kT}$. They find that at high temperature ($T >> J/k$) Eq.(2.40) reduces to

$$\ln Q_{ex} \simeq N\ln(2I+1)+\frac{1}{3}NzI^2(I+1)^2\left(\frac{J}{kT}\right)^2. \qquad (2.41)$$

For He^3 in the bcc phase, $I = 1/2$ and $z = 8$ so that the above equation reduces to

$$\ln Q_{ex} \simeq N\left[\ln 2+\frac{3}{2}\left(\frac{J}{kT}\right)^2\right]. \qquad (2.42)$$

F_{ex} is related to the partition function Q_{ex} by the relation

$$F_{ex}(v,T) = -kT\ln Q_{ex}, \qquad (2.43)$$

so that the magnetic contribution to the pressures becomes

$$P_{ex}(V,T) \simeq 3Nk\left(\frac{J}{k}\right)^2 \frac{dJ}{dV}\frac{1}{T}, \tag{2.44}$$

which may finally be put in the form

$$P_{ex}(V,T) = -\frac{3R}{V}\gamma_{ex}\left(\frac{J}{k}\right)^2\frac{1}{T}, \tag{2.45}$$

where

$$\gamma_{ex} \equiv -\frac{d\ln|J|}{d\ln V}. \tag{2.46}$$

We can see from Eq.(2.45) that in Region III the pressure is proportional to T^{-1} with the constant of proportionality being directly related to the strength of the exchange interaction J.

To obtain an expression for the free energy in the phase separation region we recall that the specific heat measurements of Edwards, et al.[24] indicated that the He^3 and He^4 atoms mix together to form a regular solution. As a consequence of this, the internal energy and entropy of the system may be written as

$$U(x,V,T) = \frac{N}{2}[xE_{44}+(1-x)E_{33}+2x(1-x)E_M], \tag{2.47}$$

$$S(x,T) = -Nk[x\ln x+(1-x)\ln(1-x)], \tag{2.48}$$

where $E_M = E_{34} - \frac{E_{33}}{2} - \frac{E_{44}}{2}$, and E_{ij} is the energy of interaction between an atom of isotope i and its nearest neighbors of isotope j.[37] For the case $x << 1$, Eqs.(2.47) and (2.48) reduce to

$$U = \frac{N}{2}(E_{33}+2xE_M), \tag{2.49}$$

$$S = -Nk(x\ln x - x). \tag{2.50}$$

When written in this form, one sees that the stable configuration of

the system depends upon the sign of E_M. If E_M is positive ($2E_{34} > E_{33}+E_{44}$), then the energy of the mixed phase is greater than that of the separated phases and the system will separate into pure isotopes at absolute zero. To find the temperature at which this separation begins, we minimize the free energy F = U-TS. For the present case, we have

$$F_{PS}(x,V,T) = \frac{N}{2}(E_{33}+2xE_M)+NkT(x\ln x-x). \tag{2.51}$$

The equation for phase separation curve is derived from the stability condition

$$\left(\frac{\partial F}{\partial x}\right)_{V,T} = 0. \tag{2.52}$$

This yields an expression for the phase separation curve in the T-x plane given by

$$x = e^{-E_M/kT} \tag{2.53}$$

where x is the concentration of the He^4 enriched phase at a temperature T and volume V. The free energy in this two phase region is obtained by substituting the expression for x given by Eq.(2.53) into Eq.(2.51). The result is the simple expression

$$F_{PS}(x,V,T) = \frac{N}{2} E_{33}-NkTe^{-E_M/kT}. \tag{2.54}$$

The internal pressure arising from the isotopic phase separation is then given by

$$P_{PS} = \frac{R}{k}\frac{dE_M}{dV} e^{-E_M/kT}. \tag{2.55}$$

Equation (2.55) shows that the size of P_{PS} is linearly related to the rate of change of the energy of mixing with density.

Finally the contribution to the pressure in the high temperature region can be obtained from the Debye free energy $F_D\left[\frac{\theta(x_o,V)}{T}\right]$ and the expression

$$P_D(x_o,V,T) = -\left(\frac{\partial F_D}{\partial V}\right)_{x,T} = -\left(\frac{\partial F_D}{\partial \theta}\right)\left(\frac{\partial \theta}{\partial V}\right), \tag{2.56}$$

or alternatively

$$P_D(x_o,V,T) = U_D(T,\theta)\ \frac{1}{\theta}\ \frac{d\theta}{dV}. \tag{2.57}$$

For solid helium $T << \theta_D$ and this becomes

$$P_D = \frac{3\pi^4 R}{5V}\left(\frac{T}{\theta}\right)^3 T\gamma, \tag{2.58}$$

where $\gamma \equiv -\frac{d\ln\theta}{d\ln V}$ is the Gruneisen parameter.

The approximate equation of state for the system is then

$$P(x,V,T)-P_o(V) = -\frac{3R}{V}\left(\frac{J}{k}\right)^2 \gamma_{ex}\ \frac{1}{T} + \frac{R}{k}\ \frac{dE_M}{dV}\ e^{-E_M/kT} + \frac{3\pi^4 R}{5V}\left(\frac{T}{\theta}\right)^3 T\gamma. \tag{2.59}$$

This equation will be used in Chapter IV to obtain the values of $|J|$, γ_{ex}, and E_M.

CHAPTER III

EXPERIMENTAL APPARATUS AND PROCEDURE

A. Introductory Remarks

The apparatus used to obtain the experimental results reported in this work incorporates many of the standard techniques of low temperature physics with enough new ideas to make it somewhat unique. It seems natural that we should describe these distinguishing features with considerable detail and present only a brief description of those sections which are conventionally used in low temperature research throughout the world. Also, as is usually true, the unique sections of the apparatus are also the most important in determining the success of these particular experiments. For these reasons we shall describe in detail the design and construction of both the potassium chrome alum salt assembly and the capacitance strain gauge, while presenting only a brief description of the helium refrigerators, vacuum systems, pressure system, and superconducting solenoids. For more details on these latter sections of the apparatus, the reader is referred to the earlier works of P. J. Walsh[38] and G. C. Straty[39] and also to the standard books[40] on the techniques used in low temperature physics.

We have also tried to follow the same philosophy in describing the manner in which the experiments were performed. Long discourses on experimental procedure from initial cooldown to final shutdown tend to

become somewhat boring, and hence we have included only those aspects of the experimental procedure which indicate the precautions taken to insure the validity of the final results.

B. Cryostat

The cryostat in which the experiments were performed is a modified version of that described by Walsh[38] and is shown schematically in Fig. (4). A more detailed drawing of the low temperature section is shown in Fig. (5). Three stages of refrigeration are required to reduce the temperature of the He^3 sample from 4.2° to 0.02°K. The temperature is lowered initially to 1.0°K by reducing the vapor pressure above a liquid He^4 bath. A further reduction to 0.3°K is obtained using a continuously operating He^3 refrigerator system. The final stage of cooling is accomplished by adiabatic demagnetization of a potassium chrome alum [$CrK(SO_4)_2 \cdot 12H_2O$] salt pill.

Helium Refrigerators

In this apparatus, the 1°K He^4 bath was contained in a cylindrical container which could be filled with liquid from the outer bath by means of a modified Hoke valve (not shown). This valve has a stem which extends through the top flange of the cryostat so that it may be operated from outside the helium dewar. To increase the thermal contact between the boiling liquid and its container, a copper spiral wound from 0.013 inch copper sheet was soldered to the bottom of the inside surface. The volume of the container is about 250 cm^3 and one filling provided 1°K operation for a period of about forty hours. A model KC-46 Kinney pump provided the necessary pumping speed to maintain

Figure 4. Schematic diagram of the apparatus.

A. Sample filling capillary

B. Exchange gas pumping line

C. He^4 bath pumping line

D. Manostat

E. He^3 refrigerator diffusion pump

F. N_2 cold trap

G. He^3 refrigerator pump

H. He^4 bath

I. He^3 refrigerator

J. Vacuum jacket

K. He^4 recovery line

L. Connection to oil and mercury manometers

M. Vacuum flange

N. Electrical Connections

O. Potassium chrome alum salt

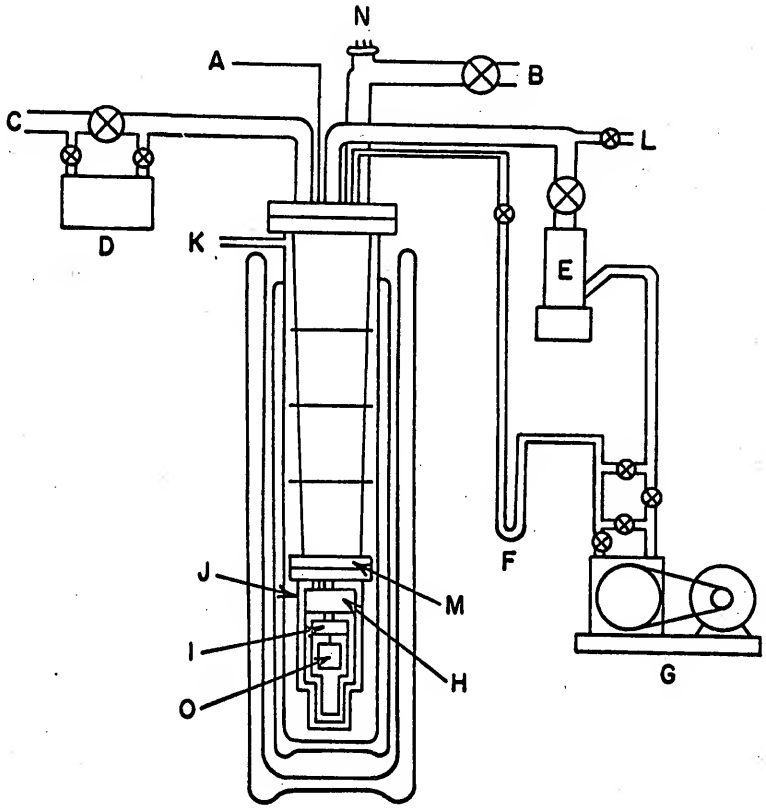
N
A
B
C
L
D
K
E
F
J
M
I
H
O
G

Figure 5. Schematic diagram of the low temperature section.

A. Various pumping lines

B. Main support and vacuum flange

C. Sample filling capillary

D. He^3 refrigerator return line

E. Electrical connections

F. Indium gaskets

G. He^4 bath

H. Vacuum chambers

I. Evaporator section of He^3 refrigerator

J. Lead heat switch

K. Nylon support tube

L. Potassium chrome alum salt

M. Demagnetization and zinc heat switch solenoids

N. Zinc heat switch

O. Sample chamber

P. 2000 #44 copper wires

Q. Vacuum jackets and radiation shields

R. Cerium magnesium nitrate thermometer

S. Primary of the mutual inductance system

T. Measuring and compensating secondaries

U. Teflon spacers

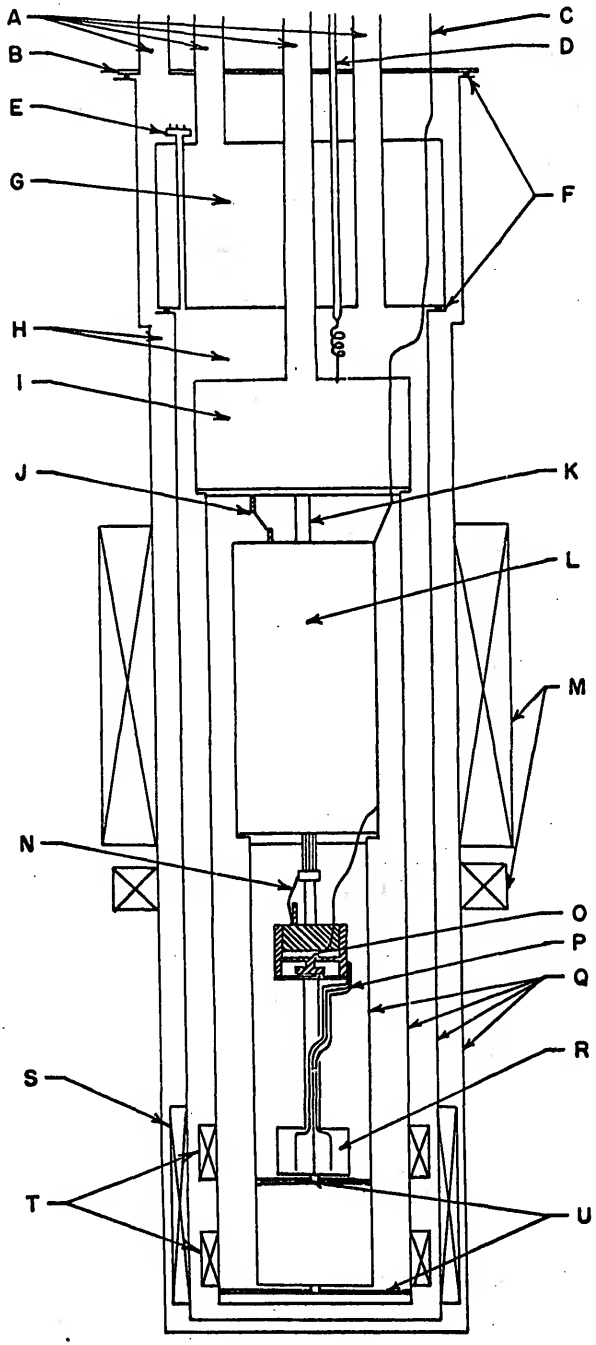
A
B
C
D
E
F
G
H
I
J
K
L
M
N
O
P
Q
R
S
T
U

the temperature at 1°K, even in the presence of substantial heat loads. Temperature control in the region between 4.2° and 1°K was accomplished by pumping through a diaphragm type manostat which allowed the pressure to be regulated to 1%. Vapor pressures were measured by mercury and oil manometers connected into the pumping line. The bottom of the container was used as a support flange for the inner vacuum jacket which also served as a 1°K radiation shield.

The He^3 refrigerator system was designed for cyclic operation. It consisted of a cylindrical container having a volume of 1 cm^3 which served as the evaporator, an NRC type B-2 oil diffusion pump in series with a Welsh Duo-Seal pump modified for closed system operation, and a constricted capillary used to produce the pressure necessary to reliquify the returning He^3 gas. A liquid nitrogen cold trap, located in the He^3 return line, was used to prevent oil vapors from entering the cryostat and possibly plugging the pressure dropping capillary. The dead volume inside the Welsh pump above the oil was used to store He^3 gas during shutdown periods. A network of mercury and oil manometers along with a CVC type GM 100 McLeod gauge was connected into the pumping line. These could be used to measure the vapor pressure of the liquid He^3 under static conditions during temperature calibrations. A carbon resistor which served as both heater and thermometer was attached to the evaporator section. By closing the return line before demagnetization it was possible to maintain a temperature of about 0.28°K at the evaporator section of the refrigerator.

Vacuum Chambers and Radiation Shields

Two vacuum chambers and four radiation shields were used to reduce the heat leak into the sample and cerium magnesium nitrate (CMN)

thermometer. An outer jacket, used to provide thermal isolation from the main He^4 bath, was attached to a flange located in the cryostat stem. An indium gasket made from 0.075 cm diameter wire was used for the vacuum tight seal. A second vacuum chamber, surrounding the He^3 refrigerator and salt system, was attached to the bottom of the 1°K bath again using an indium gasket for the vacuum tight seal. During temperature calibrations, this chamber was filled with He^4 exchange gas used to provide thermal equilibrium between the helium baths and the thermometers. The walls of the chamber were thermally grounded to the inner He^4 bath and hence provided a 1°K radiation shield for the He^3 refrigerator. A third shield, in the form of a copper plated brass cage, was screwed onto a support flange thermally grounded to the He^3 refrigerator. This cage, which contained eight small windows used for viewing the potassium chrome alum salt, completely surrounded the pill, thereby providing it with 0.3°K ambient. The construction and use of the final radiation shield will be discussed in the salt assembly section of this chapter.

Electrical leads, with the exception of the coaxial lines used for leads to the capacitor plates, were brought into the outer vacuum chamber through a small stainless steel tube. A vacuum tight glass-to-metal seal was used to bring the leads through the 1°K bath into the inner vacuum chamber. Thermal grounding to 0.3°K was accomplished by soldering the leads to small glass-to-metal seals mounted on the He^3 refrigerator. The leads were made from #36 Advance wire and a sufficient length was allowed between the refrigerators and the salt pill to provide the necessary thermal isolation. Coaxial lines were used as leads to the capacitor plates of the strain gauge wherever

possible. Where unshielded leads were used, care was taken to separate them as far as possible in order to reduce distribution capacitance. This distributed capacitance was measured with the leads disconnected at the capacitor plates, and found to be about 0.1 pf. At the working pressures encountered in these experiments, the strain gauge capacitance had a value of about 12 pf. The quantity $\frac{\Delta C}{C} = \frac{\Delta C}{C_g+C_d}$, where ΔC is the capacitance change produced by a pressure change ΔP, and C_g and C_d are the strain gauge and distributed capacitance respectively, was affected by less than 0.8% by C_d. More importantly, we observed no evidence which indicated that the value of C_d changed during the course of these experiments. In particular, it was possible to refill the liquid nitrogen bath, as well as the outer and inner He^4 baths, without affecting the value of the distributed capacitance. We are quite certain therefore that the observed capacitance changes resulted entirely from changes in the value of the strain gauge capacitance, C_g.

A discussion of the final stage of cooling and thermometry will be given after the description of the sample cell and pressure measurements.

C. The Strain Gauge

In order to make pressure measurements on samples of solid He^3, it is necessary to incorporate onto the sample cell some pressure sensing device. This is because when the sample freezes in the cell a solid plug also forms in the filling tube thereby isolating the sample chamber from any external pressure sensing devices. In these experiments a capacitance strain gauge which relates the internal pressure of

the sample to the capacitance of a parallel plate capacitor was used. The details of the strain gauge and sample cell are shown in Fig. (6).

The main section of the cell was machined from a 5/8 inch long, 7/8 inch diameter stainless steel (type 304) cylinder. A hole, 1/2 inch in diameter and 3/8 inch deep was bored into one end of the cylinder, while the opposite end was machined, as indicated in Fig. (6), to a depth of 0.205 inches. The resulting diaphragm, having a diameter of 1/2 inch and a thickness of 0.045 inches, constitutes the active element of the strain gauge. A stainless steel plug, containing a copper piece used to increase the thermal contact between the He^3 sample and the chamber walls, was designed to fit tightly into one end of the cylinder to a depth of 5/16 inch. The plug, which also contained a 0.025 inch i.d. copper capillary, was silver soldered into the main body of the chamber through two access holes drilled into the walls. Because of the snugness of the fit, no solder or flux flowed into the sample volume. The He^3 sample on which the pressure measurements were made, was located in a 1/2 inch diameter, 1/16 inch long cylindrical volume. This pancake geometry, with its large surface area to volume ratio, helps relieve any internal pressure gradients which may occur during the formation of the solid, and also helps to decrease the thermal time constant between the He^3 sample and the chamber walls. This point will be discussed in greater detail later in this chapter. A copper cylinder, containing four wells used to hold the resistance thermometers and the heater, was soldered to the steel section. This cylinder also contained a #8 copper wire which served as a thermal grounding post for attaching a zinc heat switch used to provide thermal contact between the salt pill and the sample chamber. The switch was

Figure 6. Capacitance strain gauge.

A. 2000 #39 copper wires to potassium chrome alum salt

B. Sample filling capillary

C. Zinc heat switch

D. Bakelite support

E. A #8 copper wire

F. Resistance thermometer

G. Access holes for soldering

H. Copper cylinder

I. Stainless steel chamber and plug

J. $\frac{1}{16} \times \frac{1}{2}$" diameter sample volume

K. 0.045" diaphragm

L. Capacitor plates

M. 2000 #44 copper wires to CMN thermometer

N. Bakelite support for the CMN thermometer

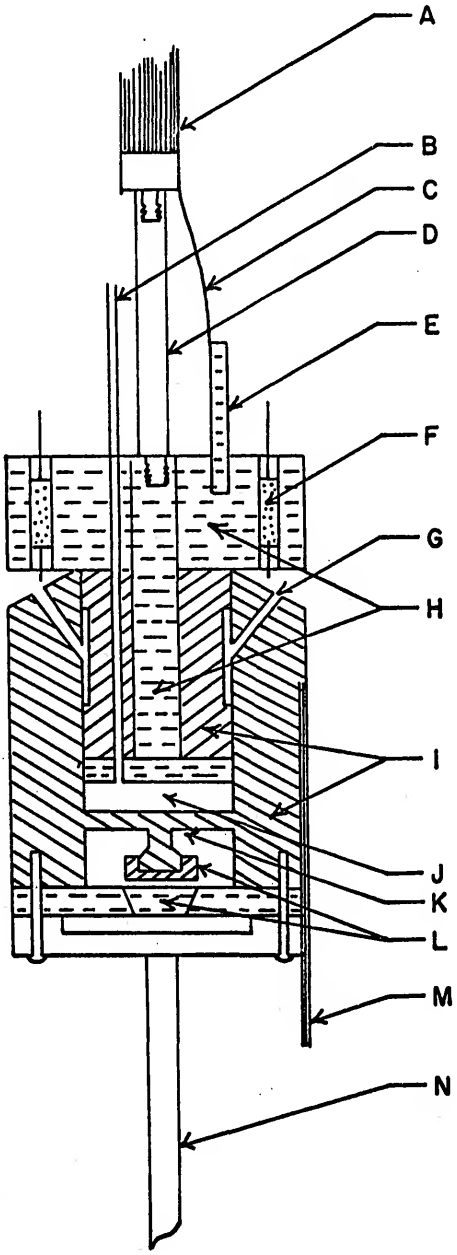
A
B
C
D
E
F
G
H
I
J
K
L
M
N

in the form of a thin foil having an area to length ratio of 0.25 mm. The cell was supported by a bakelite rod which extended from the salt pill.

The sample cell was filled with liquid through a stainless steel capillary having an o.d. of 0.033 cm and a 0.006 cm wall. A #36 Advance wire was inserted into the capillary to reduce its volume still further. A length of about 25 cm was thermally anchored to the He^3 refrigerator thereby providing a sufficiently long solid He^3 plug to prevent any slippage of material into the pressure cell. In addition to this, a length of about 20 cm was thermally grounded to the He^4 bath. No problems with plug slippage were encountered during the course of these experiments.

After the components of the chamber were soldered together, the two capacitor plates were mounted onto the strain gauge. The active plate, in the form of a circular disk having an area of 0.625 cm^2, was fastened with epoxy to the diaphragm. Tissue paper and epoxy serve to electrically insulate the plate from the chamber walls. The fixed plate was made in two sections as indicated in Fig. (6). The inner disk, having an area of 0.625 cm^2, was pressed into a tapered hole in the outer guard ring. Two layers of 0.001 inch mylar were used to electrically insulate the central plate from the outer guard ring. The plate was attached to the main section of the chamber by means of four #4-36 steel screws.

The sensitivity of the gauge to a pressure change ΔP is proportional to A/d^2 where A is the plate area and d is the plate spacing. In order to obtain a high sensitivity, it is therefore advantageous to use as small plate spacing and as large a plate area as possible.

In this experiment, the plate area was 0.625 cm^2 and the plate spacing at one atmosphere was chosen to be 0.0025 cm. To insure that the plates would not short together at the working pressure of approximately forty atmospheres, a method for setting the plate spacing devised by Straty[39] was used. After the active plate was fastened to the diaphragm, the sample chamber assembly was chucked in a lathe and light cuts were taken across both the chamber and the plate. Facing both the chamber and the plate in a single cut insured that both surfaces would be co-planar. The desired plate spacing was obtained by inserting a brass shim between the main body of the cell and the fixed plate. This particular geometry allowed both the active and fixed plates to be mounted on the same piece and thereby reduced undesirable changes in the plate spacing which arise from a differential thermal expansion of materials in the gauge. The choice of steel rather than copper as the material to be used for the main body of the strain gauge was motivated by the requirement that the diaphragm exhibit no pressure hysteresis. An earlier chamber constructed entirely from copper possessed enough hysteresis to prevent accurate determinations of the exchange energy. The present chamber has no detectable hysteresis.

The theoretical sensitivity of the gauge can be calculated from the equation for the deflection of a circular membrane fixed around its circumference. If a pressure change ΔP is distributed uniformly over its surface, the diaphragm will deflect an amount given by[41]

$$\delta = \frac{0.054\pi R^4 \Delta P}{Et^3} \qquad (3.1)$$

where

R = radius of the diaphragm in inches

t = thickness of the diaphragm in inches

E = modulus of elasticity in psi

and

ΔP = pressure change in psi.

The fractional change in capacitance $\frac{\Delta C}{C}$ is approximately given by

$$\frac{\Delta C}{C} \simeq \frac{\delta}{d} \tag{3.2}$$

where d is the plate spacing. Solving equations (3.1) and (3.2) for ΔP gives

$$\Delta P = \frac{Et^3 d\Delta C}{0.054\pi R^4 C} \cdot \tag{3.3}$$

The strain gauge capacitance has a value of about 12 pf and is measured by means of a General Radio type 1615A capacitance bridge used in conjunction with a type 1404B standard capacitor. This arrangement permits a $\frac{\Delta C}{C} \simeq 10^{-7}$ to be measured. Using the values of E, t, R and d appropriate to this chamber, one obtains a minimum detectable pressure change of 3×10^{-5} atm. The measured sensitivity at forty atmospheres was also 3×10^{-5} atm.

The data obtained in these experiments consist of a series of values of pressure as a function of temperature for a given solid sample contained within the volume of the sample cell. Although the determination of the sample pressure depends upon the deflection of the chamber diaphragm, the following considerations show that for all practical purposes the measurements are performed on constant volume samples. If we consider the pressure as a function of temperature and volume we obtain

$$dP = \left(\frac{\partial P}{\partial T}\right)_V dT + \left(\frac{\partial P}{\partial V}\right)_T dV , \tag{3.4}$$

or equivalently

$$\left(\frac{\partial P}{\partial T}\right)_V = \frac{dP}{dT} - \left(\frac{\partial P}{\partial V}\right)_T \frac{dV}{dT}. \tag{3.5}$$

By making use of the definition of the isothermal compressibility $\beta \equiv -\frac{1}{V}\left(\frac{\partial V}{\partial P}\right)_T$, Eq.(3.5) can be written as

$$\left(\frac{\partial P}{\partial T}\right)_V = \frac{dP}{dT}\left[1+\frac{1}{\beta V}\frac{dV}{dP}\right], \tag{3.6}$$

where β is the compressibility of the helium sample.

The factor $V^{-1}\frac{dV}{dP}$ is determined by the mechanical properties of the chamber and for this chamber is about 2×10^{-5} atm^{-1}. In the volume range covered by these experiments the value of β varies from about 3×10^{-3} atm^{-1} to 5×10^{-3} atm^{-1}, and hence the second term in brackets will never be greater than 10^{-2}. Thus $\frac{dP}{dT} = \left(\frac{\partial P}{\partial T}\right)_V$ to within 1% or better.

D. Pressure Measurements

Gas Handling and Pressure System

The He^3 pressure and gas handling system is shown schematically in Fig. (7). A system of three glass bulbs and two Toepler pumps was used for both storing and moving the gas. The Toepler pumps were connected through a liquid helium cold trap into one leg of a mercury U-tube pressure system. The U-tube has sufficient length so that the He^3 side could be evacuated with a pressure of one atmosphere on the opposite side. This side of the U-tube is filled with oil and connected to a dead weight gauge which served as both calibrating device and pressure manostat. A small correction was made to the pressure

Figure 7. Pressure system.

A. Vacuum line

B. Sample filling capillary

C. Oil reservoir

D. Pressure gauge

E. Dead weight gauge

F. He^4 cold trap

G. Toepler pumps

H. Mercury U-tube

I. Hydraulic pump

J. Glass storage bulbs

K. Connection to cryostat

L. N_2 cold trap

M. Nylon insulator and pressure seal

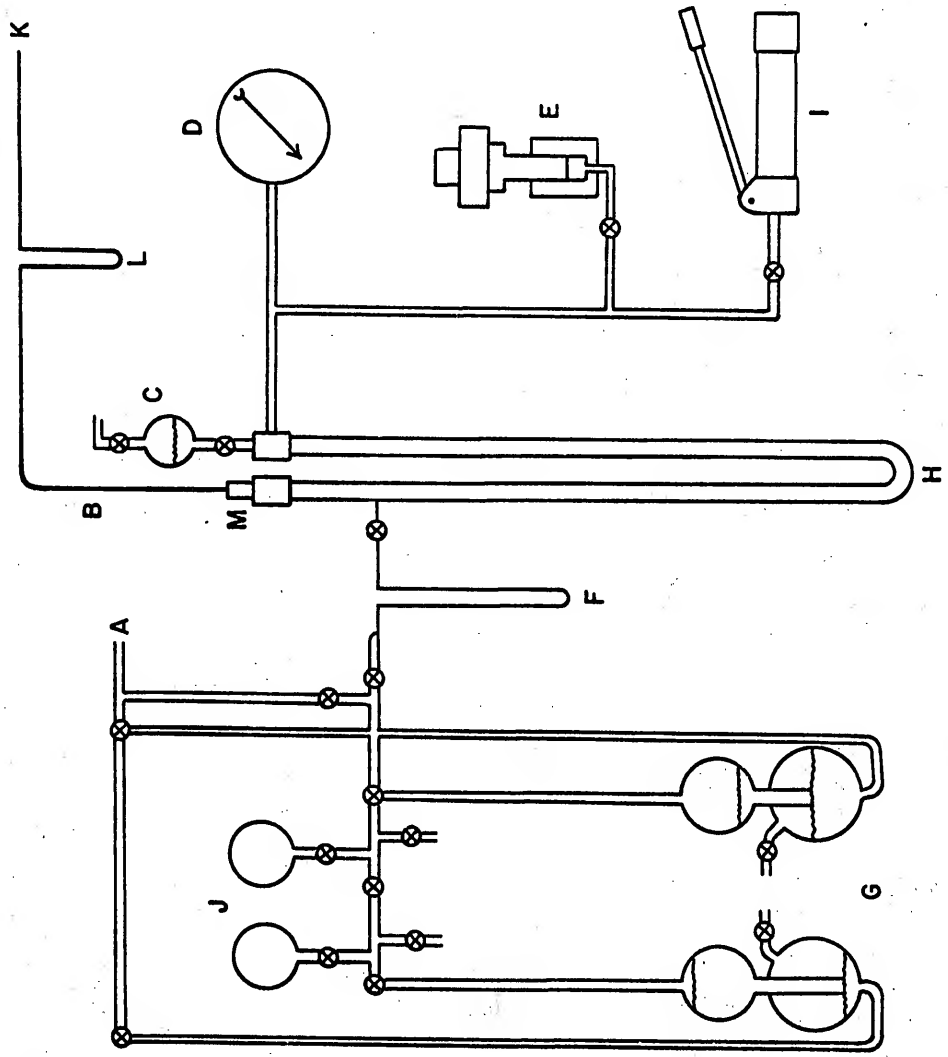
K
D
E
I
L
C
H
B
M
F
A
J
G

to compensate for the difference in the mercury levels in the U-tube. The Toepler pump connection to the gas side of the U-tube was made about 20 cm below the top so that the sample gas could be trapped in the U-tube at a low pressure. The sample filling capillary connection at the top of the tube was made through a Nylon seal. Since the U-tube was electrically insulated from its supporting structure, the mercury in the tube could then be used as a switching device to actuate an alarm which signaled the entrance of mercury into the capillary system. A small section of the external filling capillary was immersed in a nitrogen cold trap so that if a pressure leak developed in the capillary system no mercury would enter the cryostat.

Pressure Calibration and Measurement

The calibration of the strain gauge as a function of pressure was performed using the AMICO #47-2161 dead weight tester. The accuracy of this gauge is 0.05%, however, the uncertainty in the relative positions of the mercury columns limits the absolute accuracy at all pressures to about 0.03 atm. Calibration points were taken for both increasing and decreasing pressures with no detectable hysteresis.

Since the temperature at which the calibrations were made was held just above the freezing temperature of the He^3 sample corresponding to the particular density to be studied, the calibration conditions were not identical to those under which the experimental data were obtained. This was necessary to prevent a solid plug from forming in the capillary system and isolating the strain gauge from the external pressure system. To determine the effect of temperature on the capacitance of the strain gauge, a separate demagnetization was performed with the sample cell

evacuated. Aside from a small anomaly occurring at about 0.15°K, the temperature variation of the capacitance was completely negligible. This anomaly will be discussed in more detail in the following chapter since it has some effect on the quantitative accuracy of the phase separation data.

As was stated previously, the capacitance was measured by means of a General Radio type 1615A capacitance bridge used in conjunction with a General Radio 1404B standard capacitor. The GR 1615A capacitance bridge was located inside a Styrofoam container and its temperature regulated electronically to within 0.2°C. This was done in order to reduce the drift of the capacitance bridge reading which resulted from variations in the room temperature. It was determined empirically that the drift rate of the bridge reading with room temperature was about 10 af/°C.

The strain gauge capacitance was about 12 pf and could be measured to ±1 af, giving a relative sensitivity, $\frac{\Delta C}{C}$, of about 10^{-7}. The capacitance and pressure are linearly related over the range of the experimental data taken on a particular density, and hence the conversion of capacitance readings to pressure values was accomplished in a straightforward manner.

E. Potassium Chrome Alum Salt Assembly

Potassium chrome alum was chosen as the paramagnetic refrigerant because it possesses a Schottky type specific heat anomaly at about 15 m°K, and hence may be used to lower the temperature to this region. Furthermore, it has a large specific heat in the temperature range

between 0.015°K and 0.1°K, thereby permitting one to make measurements over a period of many hours, providing the residual heat leak is kept low. The size and geometry of the salt pill were chosen to utilize a previously constructed niobium zirconium solenoid.

A cross section of the salt pill and its support assembly is shown in Fig. (8). Thermal contact with the He^3 refrigerator was made by bolting the copper support flange to the bottom surface of the evaporator. Apiezon N grease was used as a thermal bonding agent. The flange was threaded so that it could be used to support the 0.3°K radiation shield which completely surrounded the salt. One end of a Nylon support tube was screwed into the bottom of the copper flange while the other end was clamped to copper wires in contact with the salt crystals. The Nylon support tube, which also served to center the salt pill inside its 0.3°K cage, had an o.d. of 0.625 cm, a wall thickness of 0.5 mm, and a length of 5 cm. A lead heat switch in the form of a thin foil having an area to length ratio of 0.1 mm thermally linked the mounting flange with the salt pill. The switch was positioned so as to be closed (normal) when the salt was fully magnetized and open (superconducting) after the initial step in the demagnetization had taken place. Before being installed, the lead was etched in warm nitric acid in an attempt to improve its on-off ratio.

The salt pill, which consisted of a mixture of 170 grams of powdered potassium chrome alum and Apiezon J oil sandwiched between sheets of #39 insulated copper wire, was assembled in a specially constructed press. The mixture was tightly compressed into a cylinder 16.0 cm long and 2.92 cm in diameter. The copper wire sheets were arranged so that those coming out the top of the salt were thermally separated by

about a 1/16-inch layer of salt from those extending out the bottom. This was done so that after demagnetization, the thermal impedence between the He^3 refrigerator and the sample would be as large as possible. The total contact area between the copper wires and the salt-J oil mixture is about 2000 cm^2. Using the specific heat and Kapitza boundary resistance data of Vilches and Wheatley,[42] we calculated a thermal time constant at 0.02°K for the salt-J oil-copper wire system of 15 minutes. A Speer grade 1002, 1/2 watt resistor having a nominal value of 220 ohms was embedded in the body of the salt and could be used to monitor its temperature during the experiment.

The salt pill itself was contained inside a phenolic tube having an inside diameter of 3.0 cm and a wall thickness of 0.8 mm. A cylindrical sheath, made from two layers of perpendicularly wound #39 insulated copper wire lightly coated with epoxy resin, was glued to the inside wall of the phenolic tube. This sheath was used to provide thermal contact between the salt crystals and a radiation shield which completely surrounded the He^3 sample and cerium magnesium nitrate (CMN) thermometer. The radiation shield, which was made by glueing two layers of #39 insulated copper wire onto a phenolic tube, was supported by a Bakelite flange as indicated in Fig. (8). The o.d. of the shield is the same as the i.d. of the copper sheath and hence they fit together very snugly. Apiezon N grease was used as the thermal bonding agent between the sheath and shield. This arrangement provided an ambient temperature of about 0.025°K for the sample and CMN thermometer system. Small cotton balls cemented to the top of the salt pill, and a Nylon spacer screwed into the bottom of the 0.025°K shield, were used to provide the final alignment of the salt in its 0.3°K cage.

Figure 8. Potassium chrome alum salt assembly.

A. Copper support flange

B. Electrical terminals

C. Lead heat switch

D. Nylon support tube

E. Sample filling capillary

F. Nylon clamp and terminal strip

G. Sheets of copper wires

H. Phenolic tube

I. Salt and J-oil mixture

J. 220 ohm Speer resistor

K. Bakelite support flange

L. Copper wire sheath

M. Brass support screw

N. 0.025°K radiation shield

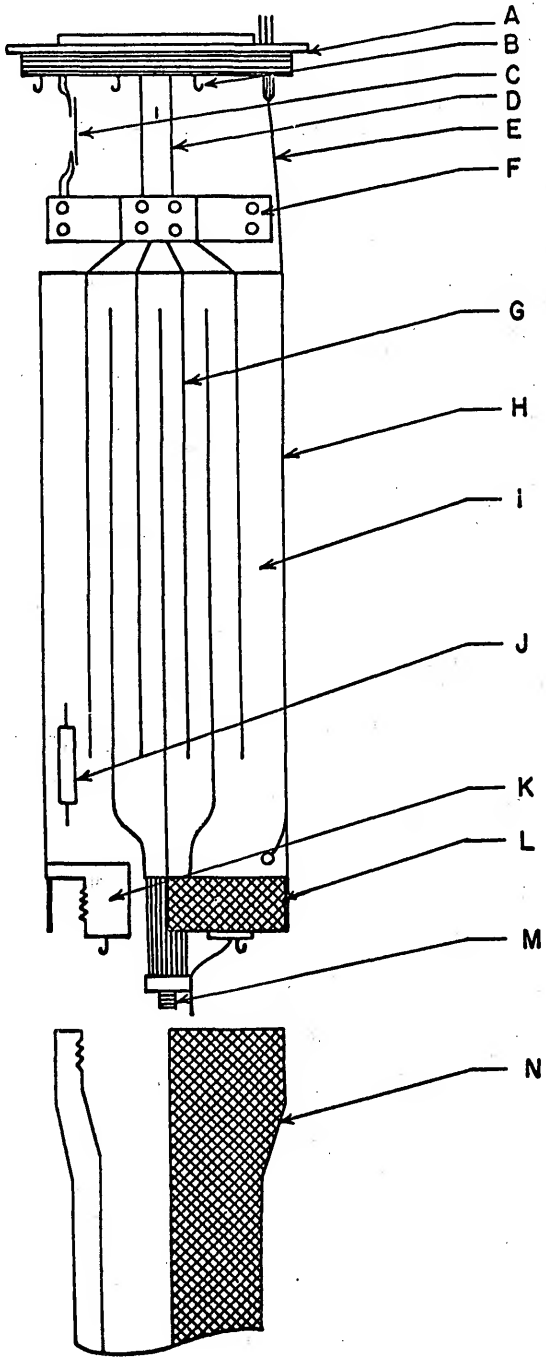
A
B
C
D
E
F
G
H
I
J
K
L
M
N

Before ending this discussion of the salt system, a few remarks concerning the residual heat leak should be made. In any of the standard books[40] on low temperature techniques, one can find formulas for calculating heat leaks due to conduction down solid supports, and radiation from surrounding walls. In most cases these calculations yield results which are correct to within about an order of magnitude only. This is due in part to the difficulty of estimating the effects of impurities and strains on the low temperature thermal conductivity of materials. Also it is difficult in many cases to include quantitatively the effects of the thermal boundary resistance between solids at low temperatures. Finally, estimates of the vibrational input from mechanical pumps and other sources are at best educated guesses. For these reasons, the author believes that the choice and dimensions of materials to be used in the design and construction of a paramagnetic salt system should be governed primarily by their successful use in similar systems. In this respect the exhaustive study of the properties of materials at low temperatures by the cryogenic group at the University of Illinois[8,42,43] has been extremely helpful.

In these experiments the sample warm up rate at 21 m°K was less than 0.1 m°K/hr. The corresponding residual heat leak was approximately 15 ergs/min. Because of the rather elaborate precautions taken to isolate the sample from vibrations and high temperature radiation, we believe the major portion of this residual heat input comes from conduction down the lead heat switch, Nylon support tube, and cotton spacers.

F. Temperature Measurements

Temperature Calibrations and Measurements

The magnetic susceptibility of powdered cerium magnesium nitrate (CMN) is known[44] to obey Curie's law, $\chi = C/T$, to temperatures as low as 6 m°K and perhaps lower. Since the constant C can be determined by measuring χ in a known temperature region, the substance is an excellent one to use for very low temperature thermometry. However because of the relatively small size of the constant C (about 1/10 as large as that of potassium chrome alum), considerable care must be taken to avoid spurious contributions to the measured susceptibility for other weakly magnetic materials present in the cryostat.

In these experiments the relative susceptibility of ten grams of powdered cerium magnesium nitrate (CMN) was used as the primary thermometer. The CMN was in the form of a right circular cylinder with the diameter equal to its height. The average dimension of the CMN crystals was about fifty microns. Two thousand #44 Formvar insulated copper wires having an area of $\sim$ 150 cm^2 were embedded in the CMN crystals with Apiezon N grease, and were used to establish thermal equilibrium between the CMN and the He^3 sample. This point will be discussed in greater detail in the following section.

The relative susceptibility was measured using a ballistic circuit shown schematically in Fig. (9). In this arrangement a measuring current, supplied by the battery, is reversed through the primary coil of the mutual inductance system M_1 which surrounds the salt pill. This induces a current pulse through the secondary which, is measured by the deflection of the ballistic galvanometer G.

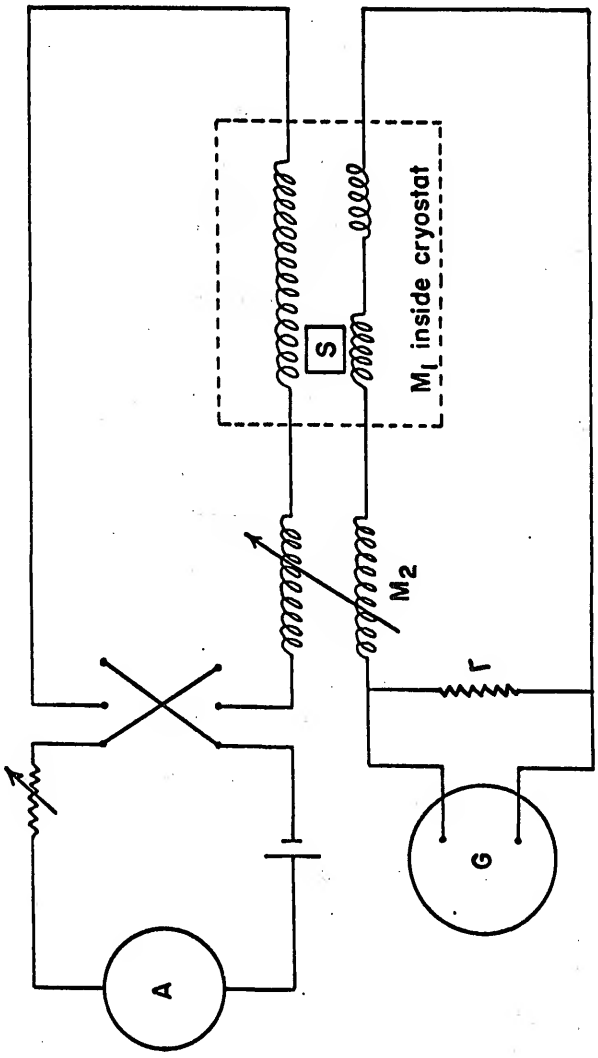

Figure 9. Simplified schematic of the dc mutual inductance circuit.

Under these conditions the size of the ballistic deflection is proportional to the susceptibility of the salt, so that we may write

$$\delta = a\chi + \delta_o = \frac{m}{T} + \delta_o . \tag{3.7}$$

The constants m and δ_o depend upon the coil geometry and the Curie constant of the CMN, and are determined by plotting δ versus T^{-1} in the 4° to 1°K calibration region.

The deflections were measured with a Leeds and Northrup type 2284D galvanometer critically damped by means of a 390 ohm shunt resistor. When used in this manner the Coulombic sensitivity and period are 5 mm/nc and 5.3 seconds respectively. Galvanometer readings were taken visually and after some experience could be estimated to tenths of a millimeter.

The mutual inductance coils are shown schematically in Fig. (10). The vertical distance between the bottom of the potassium chrome alum cooling salt and the top of the CMN thermometer salt was 9 1/2 inches. At this distance the contribution to the measured susceptibility from the potassium chrome alum is less than 0.2%.[43] The primary of the mutual inductance system is a 5 inch long solenoid located on the 1°K shield. It consisted of three tightly wound layers of #30 Formvar insulated copper wire separated from each other by Mylar sheets having a thickness of .001 inches. To avoid eddy current heating, the measuring field was varied from 5 gauss in the calibration region down to 1/2 gauss at low temperatures. The maximum power dissipated in the primary was about 1 mW and caused no measurable heating of the 1°K refrigerator. The secondary was wound on the 0.3°K shield and consisted of two nearly identical coils each 1 1/4 inches long with a

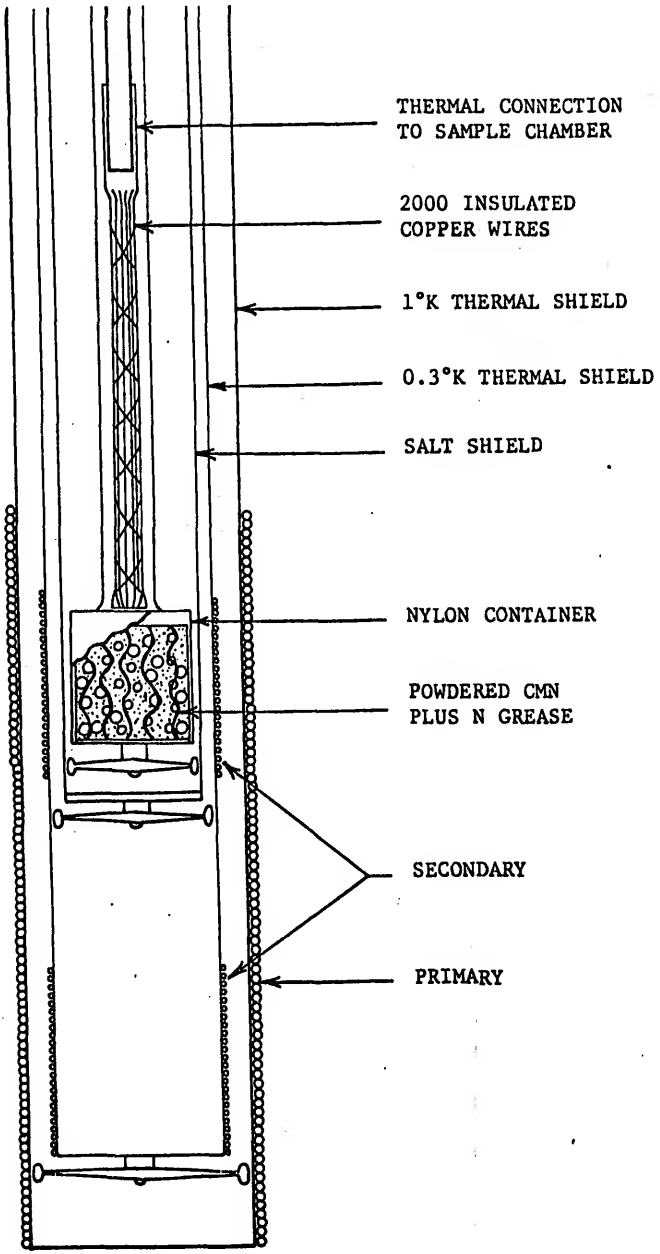

Figure 10. Schematic diagram of the CMN thermometer and the mutual inductance system. The drawing is approximately to scale.

center separation of 1/14 inches. The coils were made from 20 layers of #40 Formvar insulated copper wire. Each layer contained approximately 250 turns and successive layers were separated by one mil Mylar sheets. The wire was wound as tightly as possible in order to keep the relative positions of the turns fixed. These two coils are sometimes referred to as the measuring and compensating coils since they are connected together in opposition so that the induced EMF's will approximately compensate in the region where the salt's susceptibility is small. This is very desirable since the accuracy with which one can read the galvanometer deflections depends greatly on their size. To obtain maximum sensitivity over the entire temperature range, and also to avoid the occurrence of nonballistic deflections, two General Radio 107L mutual inductors were also used in the external circuit.

Since it generally took about thirty hours to investigate a single density and since several densities were studied, it was necessary that the mutual inductance system possess good stability over a period of several days. Temperature calibrations, taken at various times during the course of this and other experiments, indicated that this was indeed the case. It has been observed that over a period of a few weeks neither the slope nor the intercept of the deflection versus T^{-1} curve changed by more than 3%.

The CMN susceptibility was calibrated against the He^3 and He^4 vapor pressures in the temperature range from 1.1° to 3.2°K. Both He^3 and He^4 vapor pressures were used in the calibration between 1.1°K and 1.5°K, with the two calibrations agreeing to within 1%. The calibration was accomplished by first calibrating the germanium and carbon resistors

against the helium vapor pressures with the inner vacuum chamber containing 100 microns of He^4 exchange gas. The gas was then pumped away and both helium baths lowered to their working temperatures of 1.0°K and 0.3°K. The temperature of the CMN and the resistors was then controlled by a heater, and the CMN calibrated against the resistors. This was done so that the shields upon which the primary and secondary coils were mounted would be at the same temperatures during the calibration as they were during the experiment itself. Also by maintaining the shields at a constant temperature, any temperature dependent diamagnetic contributions to the susceptibility arising from the brass shields were eliminated. It is believed that the absolute temperatures are accurate to within about 1%, while below 0.08°K relative temperature changes as small as 0.1 m°K could be measured.

The carbon and germanium resistors were calibrated against the CMN and served as secondary thermometers down to 0.04°K. Both resistors exhibited good temperature reproducibility upon cycling; in particular, no measurable change in the calibration of the germanium resistor was observed even after the apparatus had been allowed to warm to room temperature and then recooled. The thermometers fit snugly in wells drilled into the copper section of the sample chamber. Thermal contact between the resistors and the copper walls was insured by melting Apiezon N grease and causing it to flow over the entire surface of the resistor.

Resistances were measured by means of a 21 cps ac resistance bridge shown schematically in Fig. (11). The phase-sensitive detector is a Princeton Applied Research type JB-4 lock-in containing a variable frequency oscillator which was used to drive the bridge circuit. The

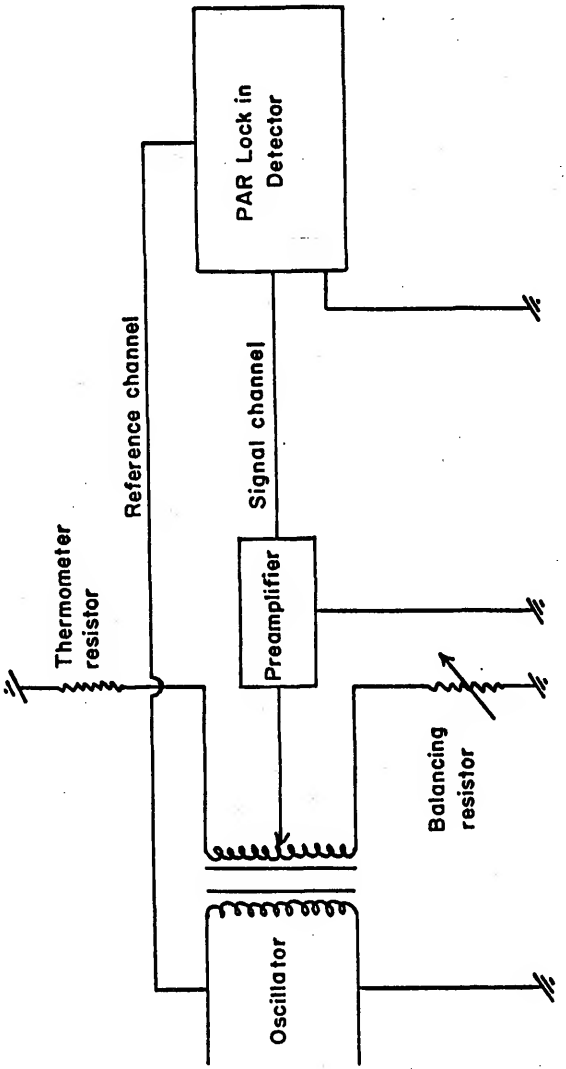

Figure 11. Simplified schematic of the ac resistance bridge.

power dissipated in the resistors was reduced from 10^{-9} W above 1.0°K down to less than 10^{-12} W at 0.04°K. Resistances could be measured to at least 0.5%, corresponding to a temperature sensitivity over the entire range of the resistors of about 0.2 m°K.

Temperature Regulation

In this apparatus a zinc foil was utilized as a thermal switch between the cooling salt and the sample chamber. This was done so that the temperature of the sample could be varied over a wide range while maintaining the temperature of the salt at a fairly constant value. With the zinc in its superconducting state, it was possible to raise the sample temperature, over a period of four to five hours, to about 0.07°K while the temperature of the salt remained below 0.03°K. This is a very desirable arrangement since it allows one to obtain several sets of pressure and temperature measurements on a given density.

The temperature of the sample was regulated by manually adjusting the current through a 33 KΩ metal film resistor located in one of the chamber wells. Regulation at the lowest temperature was accomplished with the zinc heat switch normal since only small power inputs were necessary to raise the temperature of the sample above that of the potassium chrome alum heat sink. At higher temperature, however, where the thermal gradient between the sample and salt was large, regulation was accomplished with the switch superconducting. It was also desirable to have the switch open when passing through the phase transition region, since here it was sometimes necessary to maintain a large thermal gradient for a long period of time while the mixing of the two phases took place.

Thermal Equilibrium Time between the Sample and Thermometer

In order to insure that the measured thermal expansion be produced by the helium sample alone, it is necessary to exclude all other materials from the sample volume. This means that the CMN thermometer used to measure the temperature of the He^3 spin system must be located outside the chamber. This requirement poses little problem at temperatures greater than about 0.1°K since in this region the Kapitza boundary resistance is small and hence thermal equilibrium between sample and thermometer occurs rather rapidly. However, at lower temperatures, the Kapitza resistance increases rapidly and some care must be taken to avoid producing a long thermal time constant between the sample and thermometer. A schematic diagram of the thermal path between the nuclear spins and CMN thermometer is shown below.

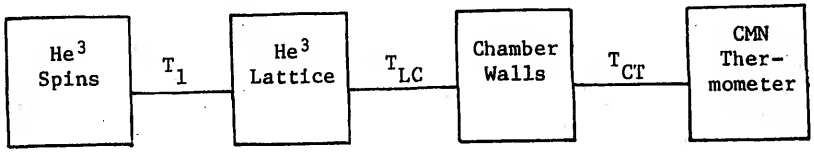

The rate at which the nuclear spins come into equilibrium with the lattice is determined by the spin-lattice relaxation time. Measurements of T_1 in the bcc phase have been performed by the Duke[26] and Oxford[27] groups down to temperatures of 0.04°K in magnetic fields of a few hundred gauss. From these results one can reasonably assume that at 0.02°K in zero magnetic field T_1 should be no longer than a few minutes for any of the densities studied in this work. Since an essentially fixed lattice temperature can be maintained for hours, the spins and lattice will have sufficient time to come into thermal equilibrium.

The CMN salt crystals and He^3 lattice come into thermal equilibrium with one another through contact with the walls of the sample chamber. The rate at which this process occurs is determined by the boundary resistance between the He^3 and the chamber walls, and between the CMN crystals and copper wires embedded in them. This Kapitza resistance between two surfaces can usually be expressed in the form

$$R_B = \frac{\Delta T}{\dot{Q}} = \frac{a}{AT^n} \tag{3.8}$$

where a and n are empirical constants, and A is the area of contact between the two surfaces. An accurate calculation of the thermal time constant for the He^3-CMN system cannot be made, chiefly because of the lack of experimental data on the Kapitza resistance of solid He^3. The measured value at 0.02°K was about five minutes. Since the drift rate at the lowest temperature is less than about 0.1 m°K per hour, we can expect the He^3 and CMN to be in excellent thermal equilibrium at all times during the experiment.

G. Solenoids

A niobium zirconium solenoid previously described by Lichti[45] was used to produce the necessary magnetic field for the demagnetization. The solenoid has a 2 inch inside diameter and is 6.88 inches long. It is equipped with a persistent switch so that it may be operated for many hours without excessive boiling of the liquid helium in the outer bath. A small resistive short was soldered across the terminals of the solenoid to give a time constant for the parallel R, L circuit of about five minutes. A Magnion type CFC 100 power supply was used to provide the current for the solenoid. A current of 17 amps in the solenoid

produced a field of 13.2 kG at the center. At 0.3°K this corresponds to an H/T ratio of 4.4×10^4 $g°K^{-1}$, a value at which the magnetization of the potassium chrome alum is essentially complete. Several attempts were made to determine the residual field of the solenoid after demagnetization. These were only partially successful so that at the present time we can only say that the residual field appears to be less than 50 G. This probably caused the final temperature to be slightly higher than might otherwise have been attained.

A small niobium solenoid also located in the outer bath was used to provide the 60 gauss necessary to actuate the zinc heat switch. The vertical distance between this solenoid and the CMN thermometer was 6 inches, and it produced no detectable field at the position of the CMN.

H. Performance of the Experiment

Sample Formation and Cooldown to 0.3°K

After the completion of the He^4 transfer, the field in the main solenoid was turned up to 13.2 kG and the current was made to persist. The He^4 exchange gas was pumped for several hours until the reading on the leakage meter of an MS9A Veeco leak detector went below an empirically determined value which indicated that the exchange gas had been essentially removed. At this point, the inner He^4 bath was filled with liquid and pumped to 1°K, He^3 gas was condensed into the evaporator section of the refrigerator and its temperature lowered to the vicinity of 0.3°K. Within about two hours, the temperature of the cell was below 2°K and the sample gas was condensed into the sample system. When the temperature of the sample was within 0.1°K of the freezing temperature

corresponding to the particular density to be studied, the refrigerators were warmed and the strain gauge calibrated against the dead weight gauge. After calibration, the pressure on the liquid was held at the desired value by the dead weight gauge and the He^3 refrigerator quickly cooled below the freezing temperature of the sample. A solid plug then formed in that section of the filling capillary thermally grounded to the He^3 refrigerator so that the desired density was obtained in the sample cell.

As the sample cooled, the melting curve was reached and the pressure in the cell dropped rapidly until the chamber became completely filled with solid. The location of the melting point was determined by the drastic change in slope which occurs when the sample leaves the melting curve and enters into the all solid region of the phase diagram. The molar volume was determined from the point of intersection of the solid isochore with the melting curve using the data of Grilly and Mills[14] and Mills, et al.[46] The temperature was then held within 0.01°K of the melting point and the solid annealed for thirty minutes. After annealing, the process of cooling the sample was allowed to continue. When the temperature reached about 0.8°K, the return valve on the He^3 refrigerator was shut. The apparatus could then be left unattended for eight to ten hours while the temperature of the salt and sample cooled to 0.3°K, at which point the inner bath was refilled and the demagnetization begun.

Demagnetization Procedure

The magnetic field was decreased exponentially, by letting it decay with the L/R time constant of about 5 min, from 13.2 kG down to about 9 kG. During this initial step in the demagnetization process

the lead heat switch became superconducting, thereby isolating the chrome alum salt from the He^3 refrigerator. The field was decreased from 9 kG to 3 kG in three steps over a period of about two hours. At this point the temperature of the sample was approximately 0.08°K, which is well below the phase separation temperature of the 600 and 1600 ppm mixtures. It was then necessary to wait for the isotopic phase separation to become essentially complete. This waiting period ranged from about thirty minutes at a molar volume of 24.0 cm^3/mole to about four hours at molar volume of 23.0 cm^3/mole. During this time, the temperature of the sample remained stationary and the onset and completion of the phase separation could be determined by watching the rate of change of the pressure with time. After determining that the phase separation was essentially complete, the demagnetization was continued. The sweep time on the power supply was adjusted so that the field would be turned down to 2000 gauss in about one hour. During this time, values of the capacitance, resistance, and ballistic deflection were taken. The sweep time of the power supply was then readjusted so that the final 2000 gauss would be turned off in approximately three hours. Again, readings of the capacitance and deflection were taken as the sample cooled. Several checks of the thermal equilibrium between the CMN thermometer and the He^3 sample were made by stopping the demagnetization process and watching the rate of change of the temperature and pressure. At all temperatures, it was found that the demagnetization proceeded slowly enough for the thermometer and sample to attain good thermal equilibrium. The lowest temperature, generally about 21 m°K, was obtained about one half hour after the final field was turned off.

No heating of the sample was done for at least another hour; during this period no detectable change in temperature occurred. Heat was then

applied to the sample and its temperature was raised to about 0.08°K over a period of about five hours. The heat was then removed and the sample allowed to recool, generally reaching a temperature in the vicinity 25 m°K. This procedure was repeated at least once for every density so that at least three sets of deflections versus capacitance readings were obtained below 0.08°K. The sample was then warmed through the phase transition region and up to the melting curve. The He^3 refrigerator was allowed to warm above the freezing temperature of the sample and the pressure calibration checked. In all cases this calibration agreed with that taken previously to within 0.01 atm.

CHAPTER IV

RESULTS AND DISCUSSION

A. Introductory Remarks

In this chapter we present values for the nuclear exchange energy and isotopic phase separation temperature obtained from three samples containing 20, 600, and 1600 ppm He^4 impurities. The data are limited to large molar volumes by the long equilibrium time for the isotopic phase separation in the 600, and 1600 ppm samples, and by the pressure sensitivity for the 20 ppm sample. The results for the volume dependence of the nuclear exchange energy, phase separation temperature, and energy of mixing, will be discussed in terms of the approximate equation of state developed in Chapter II. To facilitate this discussion, and also to indicate the relative size of the pressure changes produced by the various degrees of freedom in the solid, we present in Fig. (12) a typical isochore obtained using the 1600 ppm sample. As was done in Chapter II, the temperature scale has been divided into three regions. At temperatures greater than 0.3°K, the phonons make the largest contribution to the free energy and we find the pressure to be proportional to T^4. In the phase transition region there is a sharp increase in the pressure as the mixture separates into two phases. Finally at temperatures below $\sim$ 0.06°K, the phase separation is essentially complete, and the pressure change, $(\Delta P)_{ex}$, arising from the nuclear spin system is proportional to T^{-1}.

Figure 12. Characteristic isochore for the 1600 ppm He^4 sample. At temperatures greater than 0.4°K ΔP results primary from the lattice expansion and is proportional to T^4. At about 0.12°K there is a sharp rise in the pressure as the mixture separates into two enriched phases. Finally at temperatures below about 0.06°K the phase separation is essentially completed and the pressure changes are produced by the nuclear spin ordering in the He^3 rich phase. In this temperature region ΔP is proportional to T^{-1}.

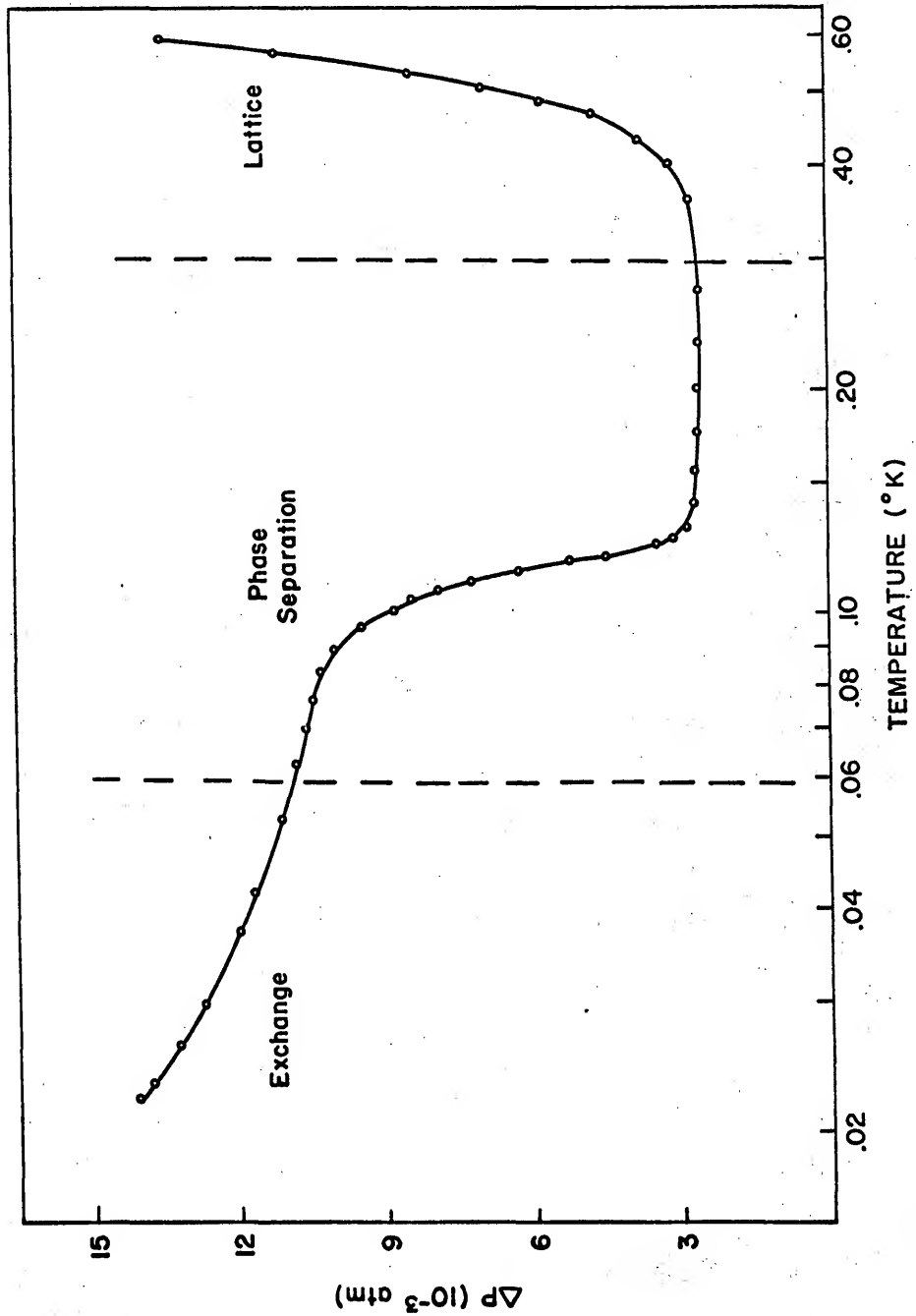
Lattice
Phase Separation
Exchange
ΔP (10⁻³ atm)
15
12
9
6
3
.02
.04
.06
.08
.10
.20
.40
.60
TEMPERATURE (°K)

Before presenting the results for the exchange energy and the phase separation temperature however, it is necessary to discuss a small anomaly in the thermal expansion of the strain gauge itself.

B. The Thermal Expansion of the Empty Cell

As previously mentioned, the pressure calibration fo the strain gauge was performed at a temperature just above the sample freezing temperature corresponding to the particular density to be studied. The calibration conditions were thus not identical to those under which the experimental data were obtained. For this reason a separate demagnetization was performed, with the sample chamber evacuated, to determine the effect of the thermal expansion of the sample chamber itself on the capacitance. The result of this demagnetization is shown in Fig. (13). In this graph the capacitance change due to the thermal expansion of the chamber has been converted into an equivalent pressure change so that its effect may be more easily compared with the pressure changes produced by the thermal expansion of the solid helium samples. It can be seen that a strange anomaly exists in the thermal expansion of the sample cell in the temperature range from 0.08°K to 0.30°K. This is also the temperature region in which the phase separation occurs, and hence the contribution to the capacitance change resulting from the thermal expansion of the chamber must be included in the analysis of the phase separation data. For the 600 ppm sample, the chamber contribution to the total capacitance change is about 10%, while for the 1600 ppm sample it amounts to approximately 4%. Below 0.06°K, the thermal expansion of the chamber is completely negligible

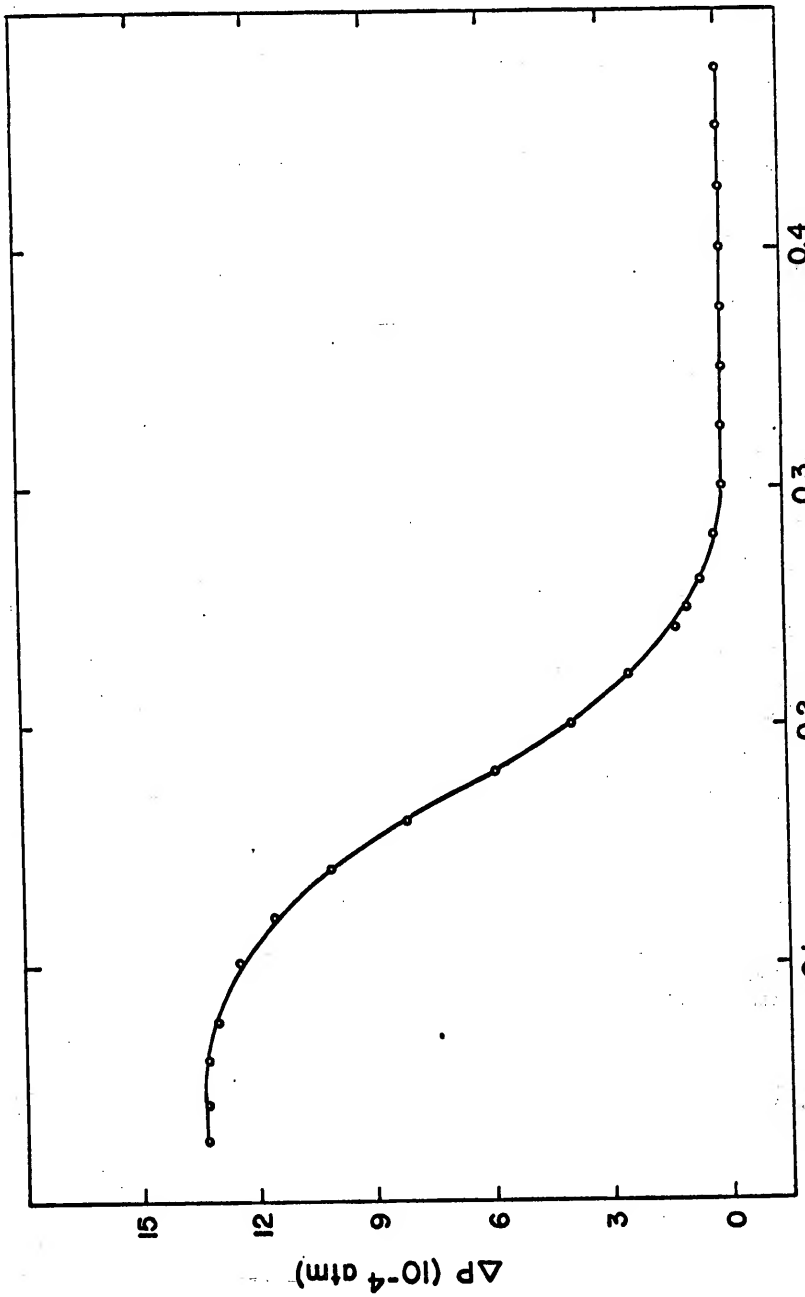

Figure 13. Thermal expansion of the empty strain gauge.

and hence does not affect the values obtained for the nuclear exchange energy.

It is interesting to speculate about the possible source of this anomaly in the thermal expansion of the sample chamber. If the thermal expansion coefficient, which is proportional to the derivative of the P versus T curve shown in Fig. (12), is plotted against temperature, the result suggests that some type of cooperative transition occurs in the chamber. A possible explanation for this behavior is that a magnetic transition takes place in the stainless steel section of the sample cell.

C. Nuclear Exchange Energy

Values of |J| for "Pure" He^3

The values given below for the nuclear exchange energy and its volume dependence are obtained from PVT data taken in the temperature region from 0.02°K to 0.06°K. In this range the He^4 impurity in the He^3 rich phase is less than 0.2 ppm, and hence the values of |J| are those for very pure He^3. The molar volumes studied in this work range from 22.8 cm^3/mole to 24.2 cm^3/mole. At smaller molar volumes, the absolute value of J becomes too small to be measured with the present pressure sensitivity.

The equation of state for dilute mixtures developed in Chapter II indicates that at low temperatures the contribution to the pressure from the nuclear spin system is given by

$$(\Delta P)_{ex} = \frac{3R}{V} \gamma_{ex} \left(\frac{J}{K}\right)^2 \frac{1}{T} \qquad (4.1)$$

where $(\Delta P)_{ex}$ is the increase in pressure relative to some arbitrary

Figure 14. The nuclear exchange contribution to the pressure, $(\Delta P)_{EX}$, versus T^{-1} for various molar volumes. The different symbols indicate different runs of that particular sample, closed symbols indicate cooling points, open symbols warming points. As explained in the text, the slopes determine the magnitude of the exchange energy, J. The sharp decrease in $(\Delta P)_{EX}$ mear $T^{-1} = 12$ for the 600 ppm samples is due to the mixing of the separated phases.

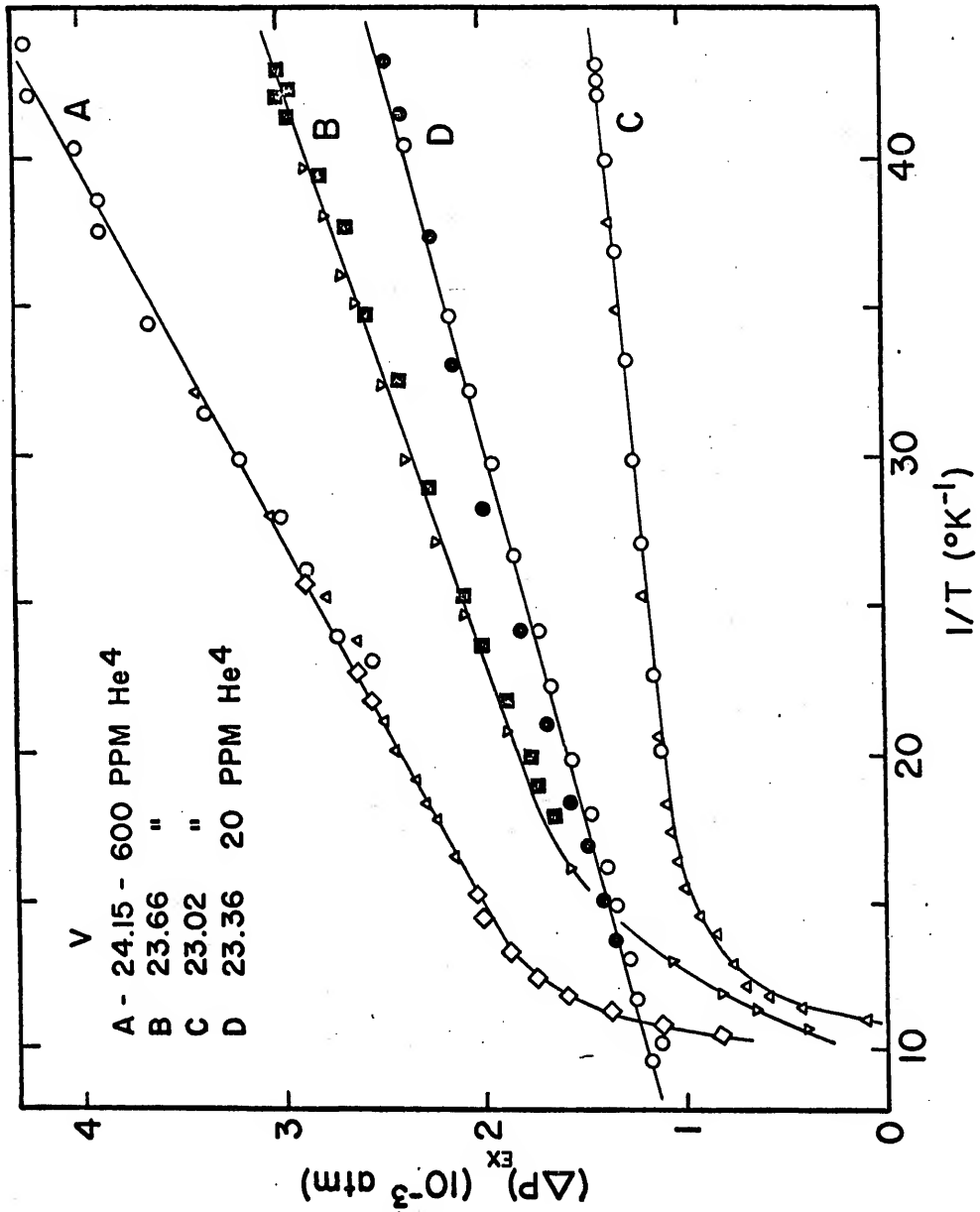
V
A - 24.15 - 600 PPM He4
B 23.66 "
C 23.02 "
D 23.36 20 PPM He4
A
B
D
C
(ΔP)ex (10-3 atm)
1/T (°K-1)
0
1
2
3
4
10
20
30
40

reference point, and

$$\gamma_{ex} = - \frac{d\ln|J|}{d\ln V}. \qquad (4.2)$$

In Fig (14) $(\Delta P)_{ex}$ is plotted versus T^{-1} for various molar volumes and He^4 concentrations. In the experimental procedure section of this work, we explained how it was possible to obtain values of P versus T for several runs on a given density. As can be seen, the data obtained on these various runs exhibit extremely good reproducibility. In view of the small sizes of the pressure changes measured, this fact is indeed comforting. The rapid decrease in $(\Delta P)_{ex}$ at a value of $T^{-1} \approx 12$ is due to the mixing of the separated phases in the 600 ppm sample.

It can be seen from Eq.(4.1) that the slopes of the $(\Delta P)_{ex}$ versus T^{-1} curves are equal to $\frac{3R}{V} \gamma_{ex} \left(\frac{J}{R}\right)^2$. Since this expression is proportional to J^2, these measurements cannot be used to determine the sign of J. Also, since it contains both J and its logarithmic derivative, a self-consistent procedure must be used to extract J from the data. The first step in this process is to assume an initial value of γ_{ex} based on the NMR data.[26,27] Equation (4.1) is then solved for $|J(V)|$ at each molar volume studied. These initial values, $|J(V)|$ can be used to compute a new, self-consistent value of γ_{ex}. The correct values of the exchange energy are then computed using Eq.(4.1) and this self-consistent value of γ_{ex}.

The values of $|J|/k$ obtained using this self-consistent procedure are presented in Table I and Fig. (15). Also shown for comparison are the results derived from NMR data,[26,27] and those calculated by Hetherington, et al.[28] The solid line fitted to the data indicates that $\gamma_{ex} = -16.4$ is valid over the density range covered by this work.

Figure 15. Nuclear exchange energy versus molar volume. The various symbols represent values of $|J|/k$ obtained using different initial He^4 concentrations. Also shown for comparison are the values of $|J|/k$ derived from the relaxation measurements of Richardson, Hunt, and Meyer (RHM); Richards, Hutton, and Giffard (RHG); and those calculated by Hetherington, Mullin, and Nosanow (HMN).

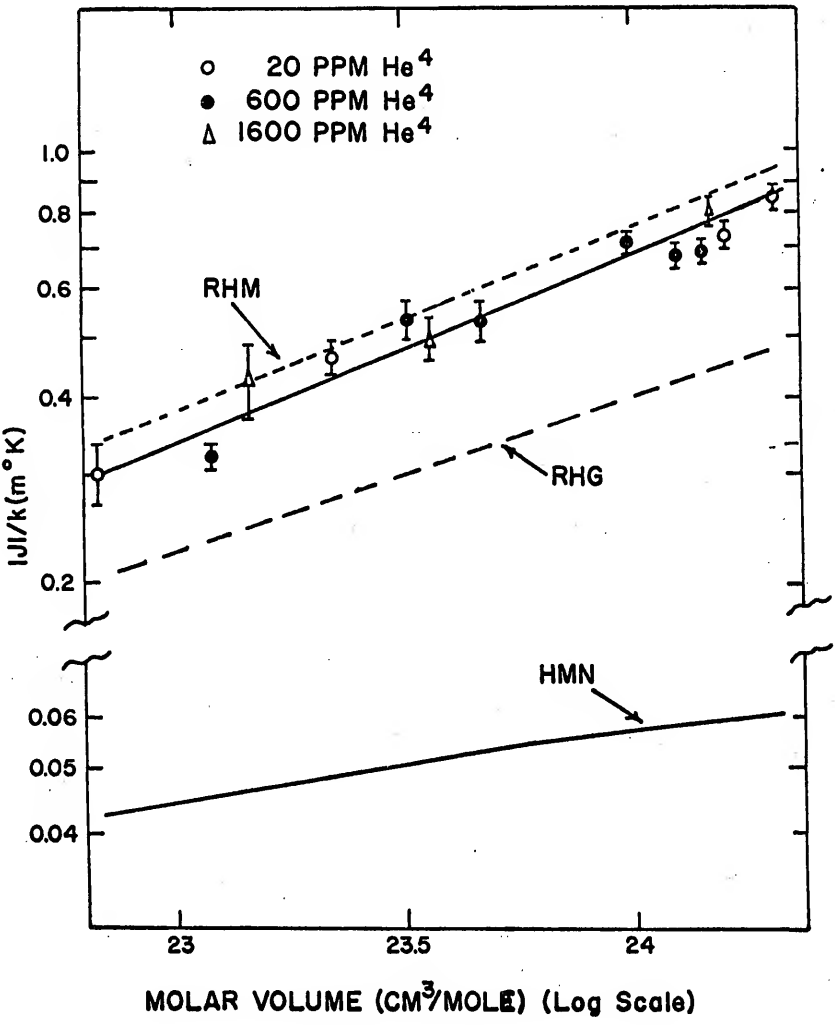
20 PPM He4
600 PPM He4
1600 PPM He4
1.0
0.8
0.6
0.4
0.2
RHM
RHG
HMN
0.06
0.05
0.04
23
23.5
24
IJI/k(m°K)
MOLAR VOLUME (CM3/MOLE) (Log Scale)

TABLE I

Smoothed Values of the Nuclear Exchange Energy in Solid He^3

V (cm^3/mole)	$\|J\|/k$ (m°K)	$T_N = 3\|J\|/k$ (m°K)
24.4	0.90	2.70
24.0	0.68	2.04
23.6	0.52	1.56
23.2	0.39	1.17
22.8	0.30	0.90

From these results it is seen that in the bcc phase $|J|/k$ is about 0.9 m°K at a molar volume of 24.4 cm^3/mole, and decreases with increasing density approximately as $\frac{d\ln|J|}{d\ln V} = 16.4$. The corresponding Néel temperature, obtained from the expression $T_N = \frac{3|J|}{k}$ varies from about 2.7 m°K at 24.4 cm^3/mole down to 0.9 m°K at 22.8 cm^3/mole.

The agreement between our values of $|J|/k$ and those derived from the NMR data of Richardson, et al.[26] is excellent. Since these pressure measurements constitute a direct method for determining $|J|$ this agreement may be interpreted as additional confirmation of the validity of the NMR formalism. Richardson[47] has suggested that the discrepancy between the Duke and Oxford values for $|J|$ arises from the latters' use of the block capillary technique to determine the molar volume of the solid. This variance in $|J|$ can be resolved if one assumes that the plug in the Oxford filling capillary slipped enough while forming the low density solid to decrease the molar volume by about 0.8 cm^3/mole. At higher densities, the values of $|J|$ determined by the Duke and Oxford workers are in better agreement, and hence Richardon's suggestion seems reasonable.

A comparison of the theoretical calculation of HMN and the experimental data indicates that while the theoretical slope agrees well with that found experimentally, the magnitude of J predicted by HMN is about an order of magnitude too small. One can understand how such a situation arises by recalling the theoretical expression for J obtained earlier,

$$J = -\frac{\hbar^2 R^2 A^2}{2m} \frac{\langle f^2(r_{ij})\rangle_x}{\langle f^2(r_{ij})\rangle} + \frac{2\langle v_{eff}(r_{ij})\rangle_x}{\langle f^2(r_{ij})\rangle}. \qquad (4.3)$$

The first term in this equation is large in magnitude and negative in sign, while the second term is of the same order of magnitude but positive in sign. One sees, therefore, that the theoretical value of J is obtained from the difference of two large numbers, each of which is accurate to about 10%. It is evident that such a situation could easily produce a relatively poor absolute value for the exchange energy, yet still yield a good value for its volume dependence.

The observed decrease in $|J|$ with increasing density is interesting and can be understood at least qualitatively on the basis of the following discussion. As the density is increased the average separation between atoms becomes smaller and intuitively one might expect the overlap region between nearest neighbor atoms to increase. This would of course increase the absolute value of the exchange energy. This in fact does not occur because, in addition to reducing the interatomic spacing, the increase in density also produces an increase in the kinetic energy of the atoms. This increase in kinetic energy is accomplished by a greater localization of the He^3 atoms to the vicinity of their equilibrium positions. In more formal language we could say that the increase in density produces an increase in the curvature and a decrease in the

extent of the wave functions describing the motions of the atoms. Since in solid He^3 the exchange energy arises as a consequence of the overlapping which occurs in the tails of these functions, any decrease in their physical extent produces a smaller absolute value for the exchange energy.

Effects of He^4 Impurities on J

Before terminating this discussion of the exchange interaction in solid He^3, a brief examination of the effects of small amounts of He^4 impurities on J will be made. The NMR data of RHG taken on a sample containing 5000 ppm He^4 indicate that the presence of a He^4 atom causes a distortion of the He^3 lattice, which in turn produces an increase in the value of J in the vicinity of the impurity site. These workers found that it was possible to express J in the form

$$J^2 = J_{bulk}^2 + J_{imp}^2, \qquad (4.4)$$

where $|J_{imp}|/k \simeq 0.1°K$ is independent of density over the molar volume range from 18.3 cm^3/mole to 20.0 cm^3/mole. If the data of Garwin and Reich,[48] obtained with a sample containing 1% He^4 impurities, are also analyzed according to Eq.(4.4) it is found that the value of $|J_{imp}|/k$ is $\simeq$ 0.5 m°K. On the basis of these two results it appears that the parameter $|J_{imp}|$ increases rapidly as the He^4 concentration is increased.

The recent magnetic susceptibility experiments of Cohen and Fairbank[49] performed on samples which contained 0.5, 100, and 3000 ppm He^4 impurities also indicate that the exchange energy increases with increasing He^4 concentration. Originally the susceptibility measurements taken on the 3000 ppm sample also indicated that the exchange energy

increased rapidly with increasing density between molar volumes of 22.6 cm^3/mole to 21.0 cm^3/mole. Subsequent experiments by the same investigators, however, have not confirmed this result, so that at the present time the question of how a small amount of He^4 impurities affects the magnetic interactions in solid He^3 remains unanswered.

D. Locus of the Zeros of the Thermal Expansion Coefficient

In Chapter II we obtained an approximate equation of state for solid He^3 given by

$$P(V,T) = P_o(V) - \frac{3R}{V}\left(\frac{J}{k}\right)^2 \gamma_{ex}\frac{1}{T} + \frac{3\pi}{5}\gamma\left(\frac{T}{\theta}\right)^3 T, \qquad (4.5)$$

where we have omitted the contribution from the isotopic phase separation. Differentiation of Eq.(4.5) with respect to temperature at constant volume gives

$$\left(\frac{\partial P}{\partial T}\right)_V = +\frac{3R}{V}\left(\frac{J}{K}\right)^2 \gamma_{ex}\frac{1}{T^2} + \frac{12\pi^4}{5}\gamma\left(\frac{T}{\theta}\right)^3. \qquad (4.6)$$

A straightforward thermodynamic derivation using the definitions of the isobaric thermal expansion coefficient $\alpha \equiv \frac{1}{V}\left(\frac{\partial V}{\partial T}\right)_P$ and isothermal compressibility $\beta \equiv -\frac{1}{V}\left(\frac{\partial V}{\partial P}\right)_T$ leads to the expression $\left(\frac{\partial P}{\partial T}\right)_V = \frac{\alpha}{\beta}$.

Goldstein[30] has pointed out that the expansion coefficient becomes zero when the negative contribution for the spin system becomes equal in magnitude to the positive contribution from the lattice. Thus, there will be a line in the P-T plane which is the locus of the zeros of the isobaric thermal expansion coefficient. By rewriting Eq.(4.6) in the form

$$\frac{\alpha}{\beta} = \left(\frac{\partial P}{\partial T}\right)_V = A_1(V)\frac{1}{T^2} + A_2(V)T^3, \qquad (4.7)$$

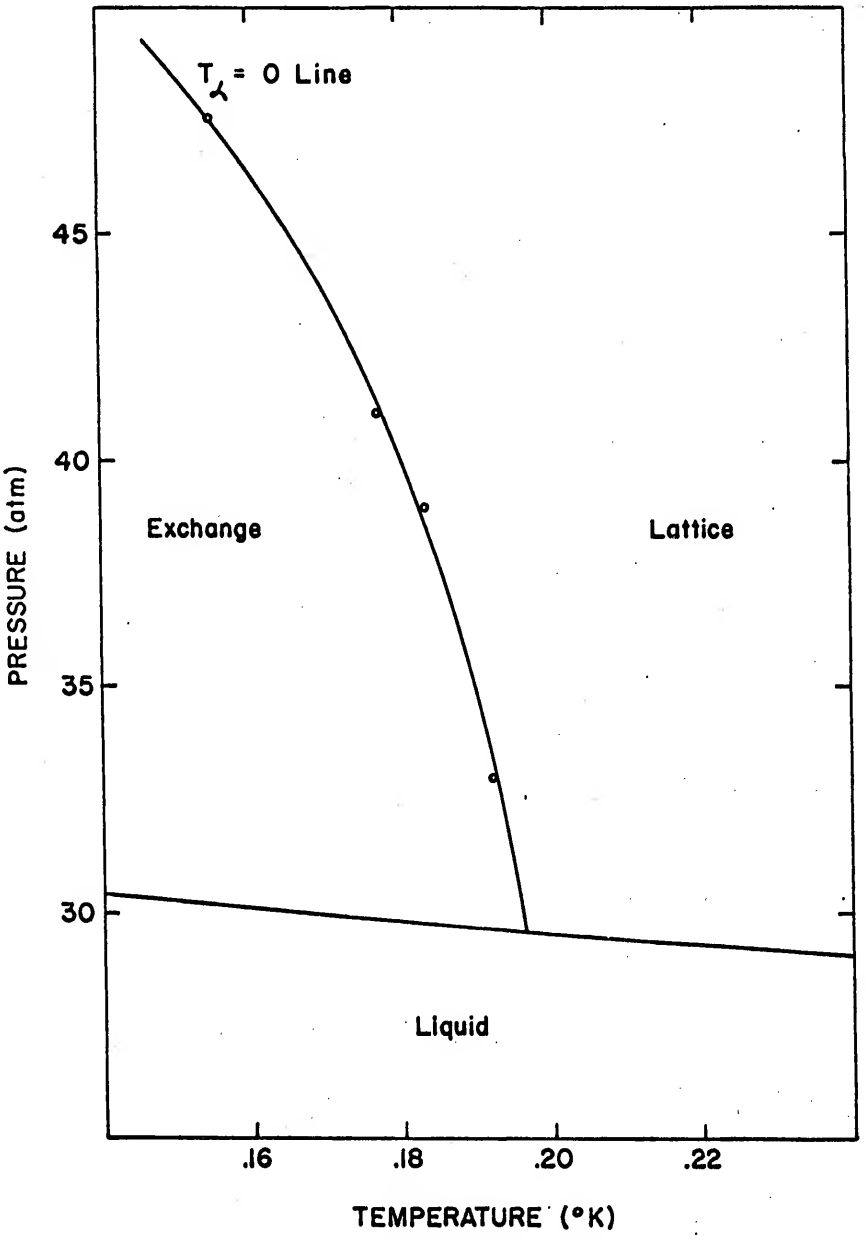

Figure 16. Locus of the zeros of the isobaric expansion coefficient.

one can see that the locus of the zeros of α is given by the relation

$$T_{\alpha=0} = \left|\frac{A_1(V)}{A_2(V)}\right|^{1/5} . \qquad (4.8)$$

We have obtained A_1 and A_2 from measurments of the slopes of the isochores in the low and high temperature limits. The result for $T_{\alpha=0}$ is shown in Fig. (16).

Roughly speaking, one can say that this locus divides the P-T plane such that at temperatures and pressures to the left of the line, the properties of the solid are determined primarily by the nuclear spins, while to the right of the $T_{\alpha=0}$ line they are determined primarily by the lattice.

E. Isotopic Phase Separation

Kinetics of the Phase Transition

One of the most striking features of the isotopic phase separation in solid He^3-He^4 mixtures is the rapid increase in the equilibrium time constant, τ, with increasing pressure. Although we have not made a detailed study of the dependence of τ on density we have noted that it increases from a value of few minutes at a molar volume of 24.2 cm^3/mole to about one hour at a molar volume of 23.0 cm^3/mole. This rapid increase in τ with density suggests that diffusion of the atoms by quantum mechanical tunnelling is the mechanism by which the separation into pure phases is accomplished. It also appears that τ is considerably longer in the cooling direction than in the warming direction, which is an indication that the atoms can mix more readily than they can separate.

The actual spacial distribution of the isotopes in the two phase region is presently uncertain. In liquid mixtures, a visually observable

bulk stratification of the two phases occurs due to the differences in mass of the two isotopes. It is highly unlikely that such a bulk separation also takes place in the solid. It seems more reasonable to picture the phase separated solid to be composed of a number of locally enriched regions, whose dimensions are very large compared to interatomic distances. In dilute solutions the number of these He^4 enriched regions is quite small, and hence the bulk properties are essentially those of a very pure He^3 system.

Pressure Dependence of the Energy of Solution and Phase Separation Temperature

The theoretical development of the isotopic phase separation phenomenon given in Chapter II was based on the assumption that the He^3 and He^4 atoms mix together randomly to form a regular solution. This model was proposed by Edwards, et al.[24] in an effort to explain the observed discontinuity in the specific heat of He^3-He^4 mixtures. The shape of the specific heat anomaly is similar to that associated with an order-disorder transition, and one interprets this as evidence for the separation of the mixture into two phases. The measurements of Edwards. et al., at a pressure of 35.8 atm., were performed on seven different He^4 concentrations ranging from 0.03 to 80%. The data indicate that the phase separation curve is symmetric about a concentration of 50% in the T-x plane.

Mullin[50] has recently developed a theory of the phase separation in solid He^3-He^4 mixtures using techniques similar to those employed by Nosanow in his study of the pure isotopes. Mullin's analysis leads to the conclusion that solid helium solutions should be nearly regular but for different reasons than those originally suggested by Edwards,

et al.[24] Two important predictions of Mullin's work are that the phase separation curve should be unsymmetrical, and that the phase separation temperature should decrease with increasing density.

In this section we present some preliminary results for the pressure dependence of the phase separation temperature, and the energy of mixing. We wish to emphasize that these results are to be regarded as tentative until confirmed by future experiments performed with mixtures containing greater amounts of He^4 impurities.

The pressure change at constant volume due to the phase separation of a dilute, regular mixture was obtained in Chapter II and is given by

$$(\Delta P)_{PS} = R \frac{d(E_M/k)}{dV} e^{-E_M/kT}, \tag{4.9}$$

where $E_M = E_{34} - \frac{E_{33}}{2} - \frac{E_{44}}{2}$ is the energy of mixing. The equation for this phase separation line has, for small He^4 concentrations, the simple form

$$x = e^{-E_M/kT}. \tag{4.10}$$

Substitution of Eq.(4.10) into Eq.(4.9) yields the following expression for $(\Delta P)_{PS}$,

$$(\Delta P)_{PS} = Rx \frac{d(E_M/k)}{dV}. \tag{4.11}$$

One can see from this equation that if $(\Delta P)_{PS} > 0$, then $\frac{dE_M/k}{dV} > 0$, and E_M should decrease with increasing density. Further by rewriting Eq.(4.10) in the form

$$T_{PS} = \frac{E_M}{k} \left| \frac{1}{\ln x} \right|, \tag{4.12}$$

it can be seen immediately that the pressure dependence of T_{PS} is similar to that of E_M.

We have measured $(\Delta P)_{PS}$ as a function of volume over the range from 23.0 cm^3/mole to 24.2 cm^3/mole for initial He^4 concentrations of 600 and 1600 ppm. The results are shown in Figs. (17) and (18). The curves shown have been obtained by a graphical smoothing procedure as follows. The capacitance values were first plotted against temperature and a smooth curve placed through the data. The contributions to the observed capacitance change from the exchange energy and sample chamber anomaly were then subtracted from this smooth curve. The resulting values for $(\Delta P)_{PS}$ versus T are those which appear in Figs. (17) and (18). We wish to emphasize that while this process is necessary to obtain the shapes of the $(\Delta P)_{PS}$ versus T curves it is not needed to establish the essential fact that $(\Delta P)_{PS}$ decreases as the density is increased. The values of $\frac{dE_M/k}{dV}$ computed from Eq.(4.11), and the measured values of $(\Delta P)_{PS}$, are shown as a function of molar volume in Fig. (19). While there is some scatter in the data, it can nevertheless be seen that $\frac{dE_M/k}{dV}$ decreases monotonically from $\sim$ 0.05°K mole/cm^3 at 24 cm^3/mole to 0.03°K mole/cm^3 at 23 cm^3/mole. Using an average value of 0.04°K mole/cm^3, and Eq.(4.12), one finds that the phase separation temperature of the 1600 ppm sample should decrease by 6 m°K between molar volumes of 24 and 23 cm^3/mole. This is in qualitative agreement with the calculation of Mullin[50] which indicates that over a similar pressure range the phase separation temperature of a 50% mixture should decrease by 0.02°K.

Finally we have determined the phase separation temperatures and energy of mixing as a function of pressure from the inflection points

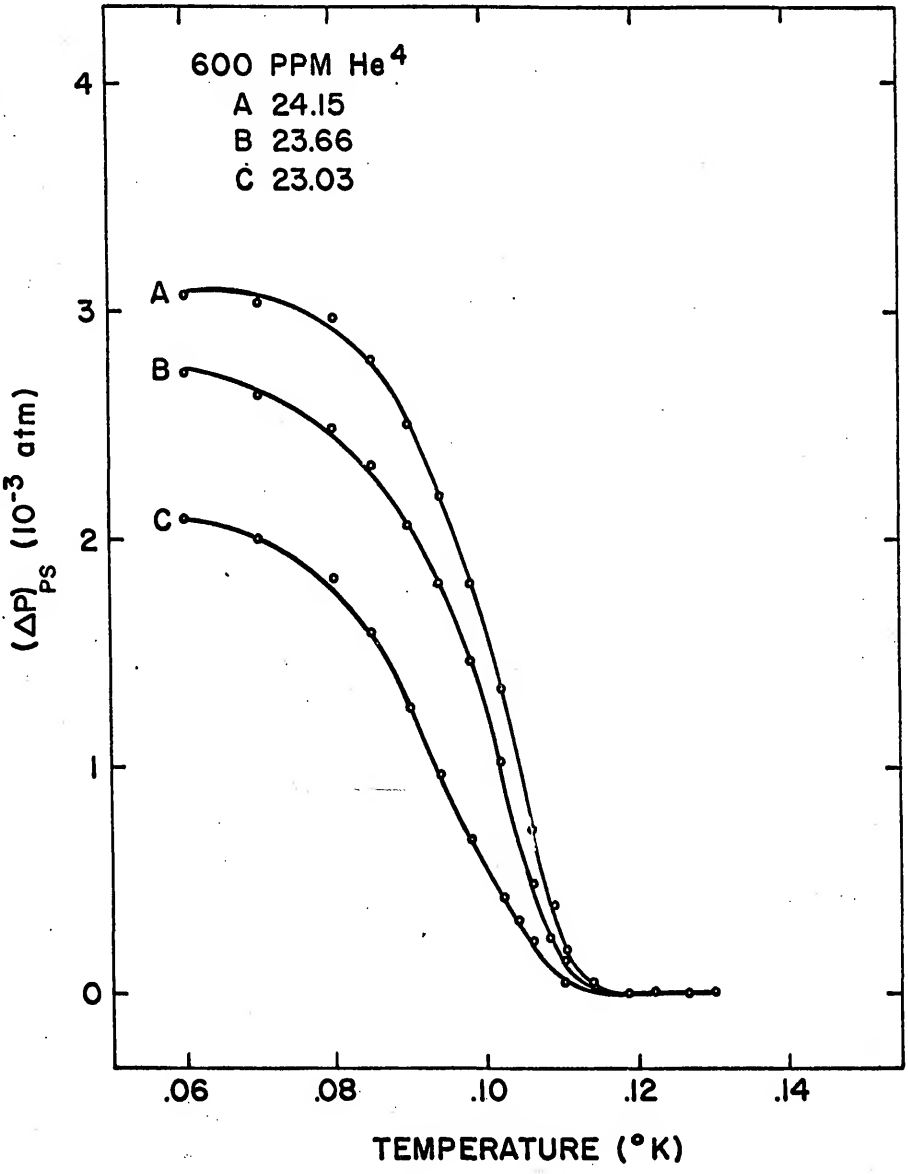

Figure 17. Pressure change, $(\Delta P)_{PS}$, due to the isotopic phase separation in the 600 ppm He^4 sample versus temperature.

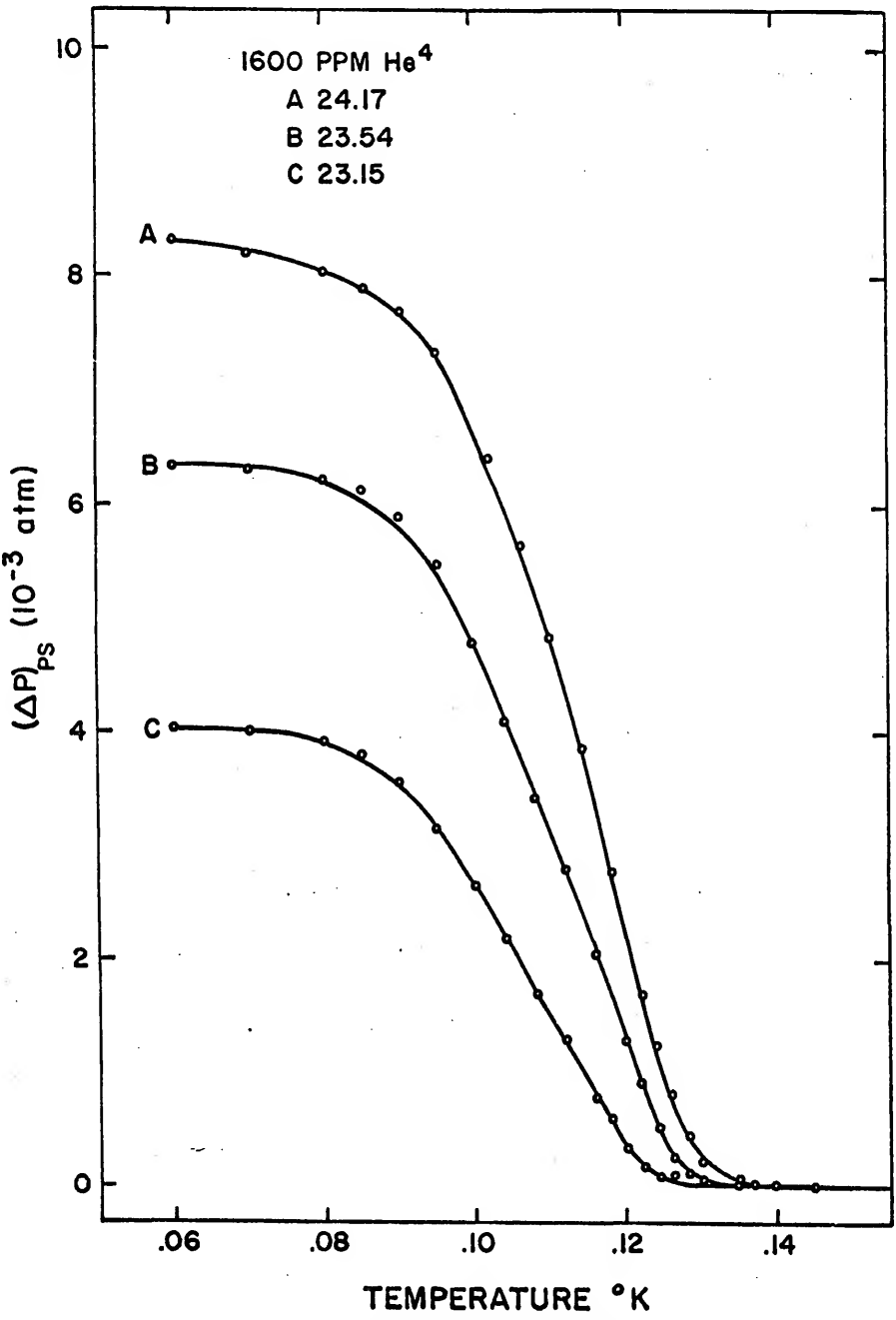

Figure 18. Pressure change, $(\Delta P)_{PS}$, due to the isotopic phase separation in the 1600 ppm He^4 sample versus temperature.

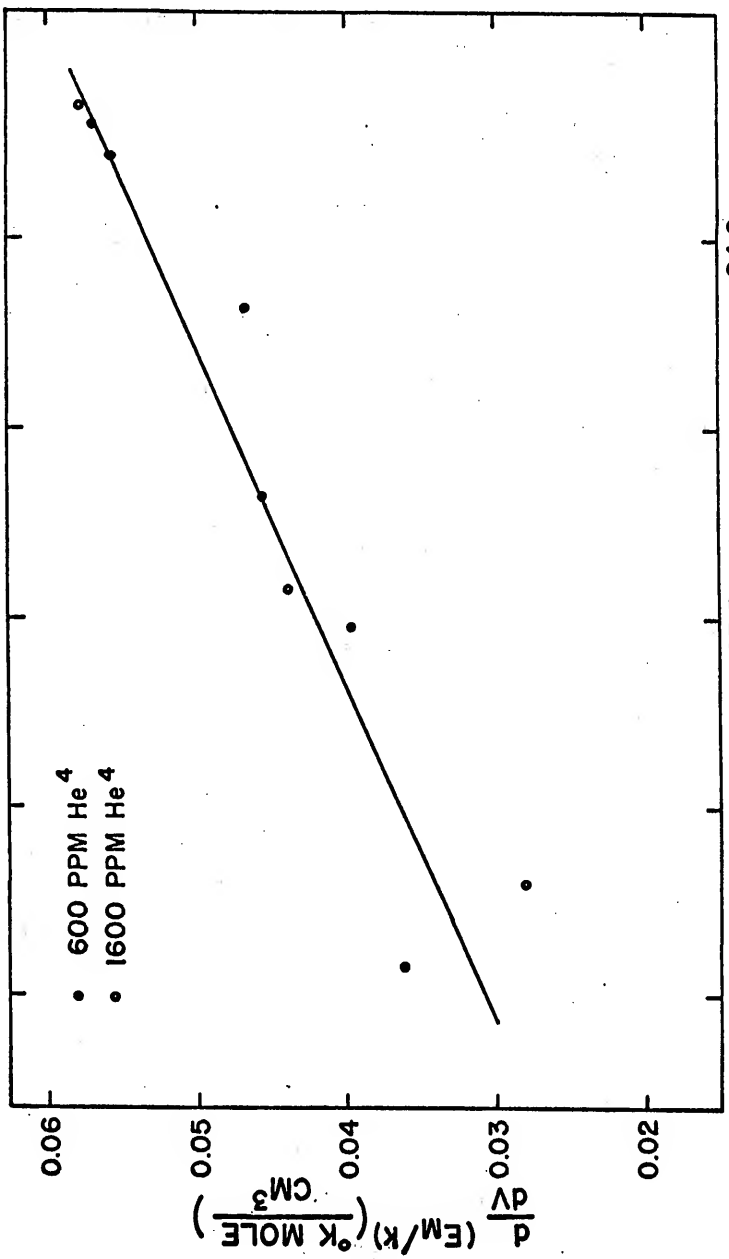

Figure 19. Plot of $\frac{dE_M/k}{dV}$ versus molar volume.

in the $(\Delta P)_{PS}$ versus T curves shown in Figs. (17) and (18). The results are shown in Fig. (20). The data posses a certain internal consistency, since the slope, $\frac{dE_M/k}{dV}$, of the E_M versus V curve in Fig. (20) is the same as that obtained using Eq.(4.11) and the measured values of $(\Delta P)_{PS}$.

At the risk of restating what has already been said, the author wishes to emphasize that the results given above are of a preliminary nature and should not be considered to possess excellent quantitative accuracy. More comprehensive experiments are presently underway which will determine not only these quantities, but also the shapes of the phase separation curve in the T-x plane. In these forthcoming experiments, the pressure resolution will be increased substantially so that the structure of the thermal expansion coefficient in the transition region will be obtained with considerable detail.

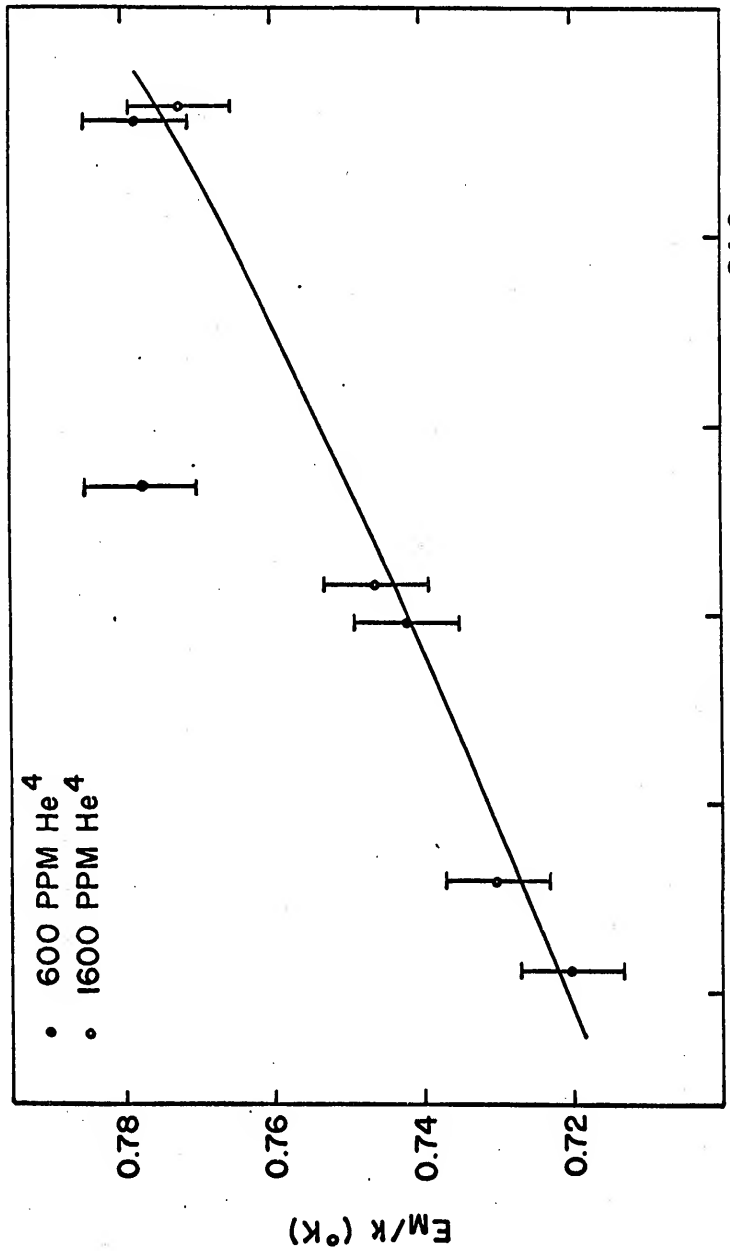

Figure 20. Energy of mixing versus molar volume. The values of E_M/k were determined from the inflection points in the $(\Delta P)_{PS}$ versus T curves, while the slope $(dE_M/k)/dV$, was determined from the magnitude of $(\Delta P)_{PS}$.

CHAPTER V

SUMMARY OF THE RESULTS

The principal aim of this investigation has been to obtain a direct determination of the nuclear exchange energy in solid He^3. This has been accomplished by measuring the contribution to the thermal expansion of the solid produced by the nuclear spin system. From these measurements it is possible to conclude that a magnetic transition will occur in low density solid He^3 at about 3 m°K, and that this temperature decreases with increasing density approximately as $\frac{d\ln T_N}{d\ln V} = 16.4$. The values obtained for the exchange energy and its volume dependence are in good agreement with those obtained earlier from the nuclear relaxation experiments of Richardson, et al.[26] at Duke University. This situation is quite gratifying since these two experimental determinations are totally independent of each other, and were obtained using entirely different techniques.

A comparison between the theoretical calculations of Nosanow and his co-workers[19,28] and our experimental results has been given. It is found that while this theory gives a good prediction for the volume dependence of the exchange energy, the absolute magnitude of J is still about an order of magnitude smaller than that determined experimentally. Because of the difficulties involved in accurately calculating the magnitude of the exchange energy, this difference is not too surprising. It is hoped, however, that future calculations, using a more accurate

ground state wave function, will tend to reduce this discrepancy between theory and experiment.

In addition to our study of the nuclear exchange energy, we have also conducted a brief investigation into the isotopic phase separation in solid mixtures containing 600 and 1600 ppm He^4 impurities. From measurements of the pressure change produced by the phase separation we have determined the pressure dependence of the equilibrium time for the phase separation, the phase separation temperature, and the energy of mixing. It has been determined that an increase in pressure from 33 atm to 45 atm increases the value of the time constant from a few minutes to about one hour, and also produces a decrease of about 5% in both the energy of mixing and the phase separation temperature.

Finally we should like to suggest a few ideas concerning the continuation of the present work. A fairly obvious extension of the present investigation would be to increase the pressure resolution and measure the exchange energy throughout the entire bcc phase. This experiment is already underway. A new chamber, with a pressure resolution about ten times greater than that used in the present experiments, will be employed to make accurate determinations of $|J|$ throughout the entire bcc phase. A second series of experiments concerned with the strength of the exchange interaction in solid He^3-He^4 mixtures is also being planned. It is expected that by varying the He^4 concentration over a reasonably wide range it will be possible to discover how the presence of diamagnetic He^4 atoms affects the strength of the exchange interaction between He^3 atoms.

At the present time it is expected that pressure measurements can be used quite successfully to determine the characteristics of the

isotopic phase separation in solid helium mixtures. Some care will have to be taken in order to insure that the measured pressure changes result primarily from the isotopic phase separation, and not from the bcc-hcp crystallographic transition which occurs in the He^4 enriched phase. The shape of the phase separation curve in the T-x plane is interesting because it is directly related to the manner in which the two isotopes go into solution. Such information, along with the density dependence of the heat of mixing, should be of considerable interest to theorists attempting to construct a suitable model for the He^3-He^4 solutions.

Finally it is expected that by using either a two stage demagnetization, or a He^3-He^4 dilution refrigerator and a single stage demagnetization, one should be able to investigate the magnetic properties of the solid at temperatures close to the transition temperature. These experiments will undoubtedly be very arduous because of the rapid increase in the thermal time constants with decreasing temperature. They would be worth the additional effort however, since their results should determine in detail the nature of the magnetic interactions in solid helium.

REFERENCES

1. F. London, Phys. Rev. 54, 947 (1938).

2. L. N. Cooper, R. L. Mills, and A. M. Sessler, Phys. Rev. 114, 1377 (1959).

3. V. J. Emery and A. M. Sessler, Phys. Rev. 119, 43 (1960).

4. A. M. Sessler, Liquid Helium, editor G. Careri (Academic Press, 1963).

5. A. L. Thomson, H. Meyer, and E. D. Adams, Phys. Rev. 128, 509 (1962).

6. B. T. Beal and J. Hatton, Phys. Rev. 139, A1751 (1965).

7. A. C. Anderson, W. Reese, and J. C. Wheatley, Phys. Rev. 127, 671 (1962).

8. W. B. Abel, A. C. Anderson, W. C. Black, and J. C. Wheatley, Physics 1, 337 (1956).

9. L. D. Landau, Zh. éksp. teor. Fiz. 30, 1058 (1956); Soviet Phys. JETP 3, 920 (1957).

10. W. B. Abel, A. C. Anderson, W. C. Black, and J. C. Wheatley, Phys. Rev. 147, 111 (1966).

11. I. Pomeranchuk, Zh. éksp teor. Fiz. 20, 919 (1950).

12. J. L. Baum, D. F. Brewer, J. G. Daunt, and D. O. Edwards, Phys. Rev. Letters 3, 127 (1959).

13. R. A. Scribner, M. F. Panczyk, and E. D. Adams, to be published.

14. E. R. Grilly and R. L. Mills, Ann. Phys. (N.Y.) 8, 1 (1959).

15. A. F. Schuch, E. R. Grilly, and R. L. Mills, Phys. Rev. 110, 775 (1958).

16. G. C. Straty and E. D. Adams, Phys. Rev. 150, 123 (1966).

17. A. F. Schuch and R. L. Mills, Phys. Rev. Letters 6, 596 (1961).

18. J. P. Franck, Phys. Rev. Letters 7, 435 (1961).

19. L. H. Nosanow, Phys. Rev. 146, 120 (1966).

20. E. C. Heltemes and C. A. Swenson, Phys. Rev. 128, 1512 (1962); H. H. Sample and C. A. Swenson, Phys. Rev. 158, 188 (1967).

21. R. C. Pandorf and D. O. Edwards, Preprint.

22. N. Bernardes and H. Primakoff, Phys. Rev. 119, 968 (1960).

23. E. D. Adams, H. Meyer, and W. M. Fairbank, Helium Three, edited by J. G. Daunt (Ohio State University Press, Columbus, Ohio, 1960).

24. D. O. Edwards, A. S. McWilliams, and J. G. Daunt, Phys. Letters 1, 218 (1962); D. O. Edwards, A. S. McWilliams, and J. G. Daunt, Phys. Rev. Letters 9, 195 (1962).

25. A. L. Thomson, H. Meyer, and P. N. Dheer, Phys. Rev. 132, 1455 (1963).

26. R. C. Richardson, E. Hunt, and H. Meyer, Phys. Rev. 138, A1326 (1965).

27. M. G. Richards, J. Hatton, and R. P. Gifford, Phys. Rev. 139, A91 (1965).

28. J. H. Hetherington, W. J. Mullin, and L. H. Nosanow, Phys. Rev. 154, 175 (1967); L. H. Nosanow and W. J. Mullin, Phys. Rev. Letters 14, 133 (1965); L. H. Nosanow, Phys. Rev. Letters 13, 270 (1964).

29. E. M. Saunders, Phys. Rev. 126, 1724 (1962).

30. L. Goldstein, Phys. Rev. 159, 120 (1967), and additional references cited therein.

31. P. Weiss, J. Phys. Radium 4, 661 (1907).

32. W. Heisenberg, Z. Physik 38, 441 (1926); 49, 619 (1928).

33. P. A. M. Dirac, Proc. Roy. Soc. (London) A123, 714 (1929).

34. J. H. Van Vleck, The Theory of Electric and Magnetic Susceptibilities (Clarendon Press, Oxford, 1932).

35. L. H. Nosanow and G. L. Shaw, Phys. Rev. 128, 546 (1962).

36. G. S. Rushbrooke and P. J. Wood, Molecular Phys. 1, 257 (1958); 6, 409 (1963).

37. J. C. Slater, Introduction to Chemical Physics (McGraw-Hill Book Company, Inc., New York, 1939).

38. P. J. Walsh, M. S. thesis, University of Florida (1963).

39. G. C. Straty, Ph.D. dissertation, University of Florida (1966).

40. For example G. K. White, Experimental Techniques in Low Temperature Physics (Clarendon Press, Oxford, 1959).

41. E. Oberg and F. D. Jones, Machinery's Handbook (The Industrial Press, New York, 1941).

42. O. E. Vilches and J. C. Wheatley, Rev. Sci. Instr. 37, 819 (1966).

43. A. C. Anderson, W. Reese, and J. C. Wheatley, Rev. Sci. Instr. 34, 1386 (1963); A. C. Anderson, J. C. Salinger and J. C. Wheatley, Rev. Sci. Instr. 32, 1110 (1961); W. R. Abel, A. C. Anderson, and J. C. Wheatley, Rev. Sci. Instr. 35, 444 (1964).

44. R. P. Hudson and R. S. Kaeser, Physics 3, 95 (1967).

45. R. D. Lichti, M. S. thesis, University of Florida (1963).

46. R. L. Mills, E. R. Grilly, and S. G. Sydoriak, Ann. Phys. (N.Y.) 12, 41 (1961).

47. R. C. Richardson, Ph.D. dissertation, Duke University (1965).

48. R. L. Garwin and H. A. Reich, Phys. Rev. Letters 12, 354 (1964).

49. H. D. Cohen and W. M. Fairbank, Preprint.

50. W. J. Mullin, Phys. Rev. Letters 20, 254 (1968).

BIOGRAPHICAL SKETCH

Michael Francis Panczyk was born on October 20, 1938, in Chelsea, Massachusetts. He obtained his secondary education in the Malden, Massachusetts public school system. In 1956, he entered Boston University and in 1960, received the Bachelor of Arts degree with a major in physics. He entered the graduate school at the University of Florida in the same year and in 1962, received the Master of Science degree with major in physics. He reentered the University of Florida in 1963, and until the present time has pursued his work toward the degree of Doctor of Philosophy.

Mr. Panczyk is married to the former Miss Mary V. Cahill and at the present time is the father of one child.

This dissertation was prepared under the direction of the chairman of the candidate's supervisory committee and has been approved by all members of that committee. It was submitted to the Dean of the College of Arts and Sciences and to the Graduate Council, and was approved as partial fulfillment of the requirements for the degree of Doctor of Philosophy.

March, 1968

E. Ruffin Jones
Dean, College of Arts and Sciences

A. Schmidt
Dean, Graduate School

Supervisory Committee:

E. W. Adams
Chairman

J. A. Scott

Jan Flowers

B. S. Thorne

R. A. Blake